Załącznik nr 3
do wniosku o przeprowadzenie postępowania habilitacyjnego
w dziedzinie nauk fizycznych w dyscyplinie fizyka

Research statement

1. First name, last name: **Mariusz Klimczak**

2. Diplomas and scientific degrees, including date of award and name, location of awarding institution, and title of PhD dissertation:
a) PhD degree in technical sciences in scope of electronics, specialty: optoelectronics,
awarded by the **Scientific Council of Faculty of Electronics and Information Technology, Warsaw University of Technology, 27th April, 2010.**
Title of PhD dissertation: „**Short-wavelength emission in neodymium and holmium doped fluorozirconate fibers**"
b) Professional title of MSc obtained in scope of program on Informatics, Automation and Robotics, Electronics and Telecommunications in scope of electronics - optoelectronics,
Faculty of Electronics and Information Technology, Warsaw University of Technology
29th, October, 2004
Title of MSc dissertation: „**UV emission in ZBLAN glasses activated with Nd^{3+} ions**"
c) Professional title of Engineer obtained in scope of program on Informatics, Automation and Robotics, Electronics and Telecommunications in scope of optoelectronics,
Faculty of Electronics and Information Technology, Warsaw University of Technology
11th, October 2002
Title of Engineering project: „**Laboratory model of Nd:YAG microlaser with second harmonics generation, pumped with a laser diode**"

3. Information on previous and current employment in research institutions

2013 – assistant professor (adjunct), Institute of Electronic Materials Technology in Warwsaw, Glass Department
        postdoc in scope of TEAM project awarded by Foundation for Polish Science

2010-2013 – research assistant, followed by adjunct, Institute of High Pressure Physics, Polish Academy of Sciences

4. Scientific achievement as per art. 16, p. 2 law dated on 14 March 2003 on the scientific degrees and on the scientific titles and on the degrees and the title in scope of arts (Polish: Dz. U. nr 65, poz. 595 ze zm.):
    a) the title of the scientific achievement
        Cycle of research papers related in scope and subject: **Impact of the dispersion characteristics of the nonlinear medium and of the initial pump pulse condition on the spectral and coherence properties of the supercontinuum**

    b) (author/authors, title/titles of papers, year of issuing, name of publisher)

MK-1. Stepniewski, G., Klimczak, M., Bookey, H., Siwicki, B., Pysz, D., Stepien, R., Kar, A.K., Waddie, A.J., Taghizadeh, M.R., Buczynski, R., Broadband supercontinuum generation in normal dispersion all-solid photonic crystal fiber pumped near 1300 nm, (2014) Laser Physics Letters, 11 (5), art. no. 055103. DOI: 10.1088/1612-2011/11/5/055103, IOP Publishing
Contribution of the applicant: the preparation of the numerical model and performing numerical simulations, the analysis, interpretation and discussion of all experimental and theoretical results, as well as writing and correction of the manuscript, 35%.

MK-2. Klimczak, M., Siwicki, B., Skibiński, P., Pysz, D., Stępień, R., Heidt, A., Radzewicz, C., Buczyński, R., Coherent supercontinuum generation up to 2.3μm in all-solid soft-glass photonic crystal fibers with flat all-normal dispersion, (2014) Optics Express, 22 (15), pp. 18824-18832. DOI: 10.1364/OE.22.018824, OSA Publishing
Contribution of the applicant: numerical simulations, interpretation and analysis of experimental results, writing and corrections of the manuscript, 40%.

MK-3. Sobon, G., Klimczak, M., Sotor, J., Krzempek, K., Pysz, D., Stepien, R., Martynkien, T., Abramski, K.M., Buczynski, R., Infrared supercontinuum generation in softglass photonic crystal fibers pumped at 1560 nm,
(2014) Optical Materials Express, 4 (1), pp. 7-15. DOI: 10.1364/OME.4.000007, OSA Publishing
Contribution of the applicant: numerical simulations, interpretation and analysis of experimental results, writing and corrections of the manuscript, 30%.

MK-4. Klimczak, M., Stepniewski, G., Bookey, H., Szolno, A., Stepien, R., Pysz, D., Kar, A., Waddie, A., Taghizadeh, M.R., Buczynski, R., Broadband infrared supercontinuum generation in hexagonal-lattice tellurite photonic crystal fiber with dispersion optimized for pumping near 1560 nm, (2013) Optics Letters, 38 (22), pp. 4679-4682. DOI: 10.1364/OL.38.004679, OSA Publishing
Contribution of the applicant: the preparation and running of the numerical simulation, the analysis, interpretation and discussion of all the experimental and theoretical results and writing and corrections of the manuscript, 30%.

MK-5. Klimczak, M., Siwicki, B., Skibinski, P., Pysz, D., Stepien, R., Szolno, A., Pniewski, J., Radzewicz, C., Buczynski, R., Mid-infrared supercontinuum generation in soft-glass suspended core photonic crystal fiber,
(2014) Optical and Quantum Electronics, 46 (4), pp. 563-571. DOI: 10.1007/s11082-013-9802-1, Springer US
Contribution of the applicant: numerical simulations, interpretation and analysis of experimental results, writing and corrections of the manuscript, 30%.

MK-6. Klimczak, M., Soboń, G., Abramski, K., Buczyński, R., Spectral coherence in all-normal dispersion supercontinuum in presence of Raman scattering and direct seeding from sub-picosecond pump, (2014) Optics Express, 22 (26), pp. 31635-31645. DOI: 10.1364/OE.22.031635, Springer US
Contribution of the applicant: design of the experimental setup, analysis of experimental results, writing and corrections of the manuscript, 40%.

MK-7. Klimczak, M., Soboń, G., Kasztelanic, R., Abramski, K.M., Buczyński, R., Direct comparison of shot-to-shot noise performance of all normal dispersion and anomalous dispersion supercontinuum pumped with sub-picosecond pulse fiber-based laser,
(2015) Scientific Reports 5, 19284, DOI: 10.1038/srep19284, Nature Publishing Group
Contribution of the applicant: the concept and plan of the research work, numerical simulations, interpretation and analysis of all obtained results, writing and corrections of the manuscript, 40%.

MK-8. Klimczak, M., Komolibus, K., Piwoński, T., Siwicki, B., Pysz, D., Stępień, R., Ochalski, T., Buczyński, R., Impact of steepness of pump temporal pulse profile on spectral flatness and correlation of supercontinuum in all-solid photonic crystal fibers with flattened normal dispersion, (2014) Journal of Optics (United Kingdom), 16 (8), art. no. 085202. DOI: 10.1088/2040-8978/16/8/085202, IOP Publishing
Contribution of the applicant: the concept and plan of the research work, preparation and performing of the theoretical part of research, interpretation and analysis of all obtained results, writing and corrections of the manuscript, 51%.

MK-9. Siwicki, B., Klimczak, M., Stępień, R., Buczyński, R., Supercontinuum generation enhancement in all-solid all-normal dispersion soft glass photonic crystal fiber pumped at 1550 nm, (2015) Optical Fiber Technology Vol. 25, pp. 64–71, DOI: 10.1016/j.yofte.2015.08.001, Elsevier
Contribution of the applicant: preparation of the numerical model, supervising of the research, discussion of results and corrections to the manuscript, 40%.

MK-10.Siwicki, B., Klimczak, M., Soboń, G., Sotor, J., Pysz, D., Stępień, R., Abramski, K., Buczyński, R., Numerical simulations of spectral broadening in all-normal dispersion photonic crystal fiber at various pump pulse conditions, (2015) Optical Engineering, 54 (1), art. no. 016102, DOI: 10.1117/1.OE.54.1.016102, SPIE
Contribution of the applicant: the concept of work, preparation of the numerical model, supervising of the numerical simulations, analysis of results, 40%.

MK-11.Buczyński R., Klimczak M., Stefaniuk T., Kasztelanic R., Siwicki B., Stępniewski G., Cimek J., Pysz D., Stępień R., Optical fibers with gradient index nanostructured core, (2015) Optics Express Vol. 23, Issue 20, pp. 25588-25596, doi: 10.1364/OE.23.025588, OSA Publishing
Contribution of the applicant: fabrication of the physical fibers, measurements of the supercontinuum spectra, analysis and discussion of all results, writing and corrections of the manuscript, 30%.

c) discussion on the scientific goal of work and presentation of the obtained results, including discussion of the possible applications

Introduction

During the 3-year period prior to submitting of this application, the applicant has been employed at Institute of Electronic Materials Technology in Warsaw (**ITME**), as an assistant professor (adjunct). The applicant was involved in realization of the TEAM project of the **Foundation for Polish Science**, project title "Novel light sources based on photonic crystal fibers with nanostructured cores" (nr TEAM/2012-9/1) co-financed by the European Regional Development Fund, Operational Program Innovative Economy 2007-2013. The Principal Investigator in that project was Ryszard Buczyński, PhD DSc, prof. ITME.

The main axis of the research paper cycle presented by the applicant is the impact of the dispersion characteristics of the nonlinear medium and of the initial pump pulse condition on the spectral and coherence properties of the supercontinuum. The cycle includes papers cited in the text as [**MK-1 ... MK-11**]. When selecting the research papers to be included in the cycle, the applicant was motivated with the intent to present his work in a possibly widest scope of conducted research. Therefore, the cycle begins with the papers, where the applicant, together with collaborators, has for the first time demonstrated generation of a coherent, octave-spanning, near-infrared supercontinuum in all-solid glass photonic crystal fibers with flattened profile of normal dispersion [**MK-1,MK-2**]. The papers [**MK-3...MK-5**] summarize results on the development of the technology of highly nonlinear glasses with transmission window extending to about 5 µm. These works are not focused directly on the idea of showing breakthrough supercontinuum bandwidth. The significance of these results and importance to the cycle of the applicant's research, stems from the demonstration of successful fabrication of highly nonlinear photonic crystal fibers, using technologically demanding glasses, with an unique layout of the photonic lattice (which demonstrates wide flexibility in designing of the dispersion profile) and with pump laser damage

threshold high enough, to allow pumping with relatively high energy pulses from new, robust fiber-based picosecond lasers operating at about 1560 nm. These results represent a step towards designing and fabrication of fibers for stable supercontinuum generation covering the attractive mid-infrared range of wavelengths.

In the light of the available state-of-the-art, pumping with pulses lasting over 100-300 fs (depending on the dispersion profile of the nonlinear fiber) favors the effect of noise amplification, which results in supercontinuum dramatically losing the phase coherence [1,2]. Papers [**MK-6,MK-7**] contain results of theoretical and experimental work on the new means to preserving of the phase coherence of supercontinuum spectrum obtained in the normal dispersion range of wavelengths (of a nonlinear fiber). **Specifically, the applicant has for the first time demonstrated, that a higher order mode in an optical fiber, can successfully seed the fundamental mode of the fiber, leading to efficient phase noise suppression and reduction of the spectral intensity fluctuations.** These results were obtained in photonic crystal fibers with a special design of the photonic lattice layout. The works [**MK-8,…,MK-10**] contain results of simultaneously conducted theoretical research on the impact of the initial condition parameters (i.e. the pump pulse parameters) on the spectral and coherence characteristics of the supercontinuum spectrum. The results presented in these papers were used by the applicant and co-workers, as they appeared, in the designing and fabrication of the photonic crystal fibers investigated during the passing three years of work. The paper [**MK-11**] on the other hand, demonstrates a completely new approach to the designing and fabrication of structured optical fibers with predetermined modal and dispersion properties, by the use of the nanostructuring of the core area. These results open up new possibilities in the future research work of the applicant, which would be focused on new effects in nonlinear optics, enabled by spatio-temporal properties of waveguiding nonlinear media [3].

Whenever there is mentioned the applicant's team or group, it is meant the research group at the Glass Department, Institute of Electronic Materials Technology in Warsaw; the group is headed by Ryszard Buczyński PhD DSc prof. ITME. Members of the group, apart from the group head and the applicant, are chief technologists dr Ryszard Stępień (glass synthesis) and Dariusz Pysz (fabrication of Photonic crystal fibers), the technicians, and PhD students: Jarosław Cimek (technology of highly nonlinear glasses for fabrication of structured fiber optics), Grzegorz Stępniewski and Bartłomiej Siwicki (characterization, designing and fabrication of photonic crystal fibers, analysis of nonlinear optical effects in photonic crystal fibers). R. Buczyński is supervising all three PhD students. The applicant is the assistant supervisor for Mr. Stępniewski and Siwicki. Since the beginning of the TEAM project, the group has also included Mrs. Agnieszka Szołno, until her tragic passing in September 2013. Research interests of Mrs. Szołno included designing of nonlinear photonic crystal fibers and supercontinuum generation.

State-of-the-art at the beginning of the applicant's work with nonlinear fiber optics

The pace of research work in the disciplines making use of the techniques such as optical coherence tomography (OCT) [4], generation of ultra-stable optical frequency combs [5], as well as other areas of research concentrated on exploring the processes, which occur over very short timescales or with very low repeatability [6], stimulates the development of new sources of radiation. Such sources should be characterized with high brightness, broad spectral coverage of generated radiation, and – what is of paramount importance – high phase coherence and spectral coherence. Imaging of biological tissue in OCT benefits from the change of probing wavelength from 1.3 to 1.7 µm, where the scanning beam experiences less scattering and stays away from water absorption [7]. Moreover, application of a shot-to-shot repeatable supercontinuum source, delivering spectrum contained entirely within the normal dispersion range of wavelengths of the nonlinear fiber, allows to increase the imaging penetration depth and to improve the signal-to-noise rate (SNR) by 10 dB [8]. Similar advantages are obtained with a broadband source operating at a wavelength of around 2 µm and longer for OCT imaging of non-biological matter [9]. A coherent supercontinuum source in the role of an optical pump for an optical frequency comb, in one of the first reports, enabled obtaining 20 channels distributed across a 10 GHz bandwidth around wavelength of 1558 nm and within 6 dB dynamical range. Results were also published demonstrating near a factor of 20 increment of the number of channels and in a twice narrower bandwidth,

4

also in the third telecommunication window [10]. The benefits of stability of a broadband, pulsed source were also demonstrated in context of phase shift keying communications (PSK) [11]. Bit error rate (BER) was compared here in a transmission experiment, where a frequency comb source used as the reference was pumped with either anomalous dispersion-pumped supercontinuum or an all-normal dispersion supercontinuum. The use of the latter source resulted in negligible influence of BER on PSK transmission.

This brief list of possible research applications of coherent broadband sources, popularly referred to as supercontinuum (other names such as "white laser" or "white light" are also in use, despite their imprecise or contradictory nature), are by no means exhaustive. The given list was purposely limited to the situations, where minimization of phase and intensity fluctuations is critical. Admittedly, there are numerous applications, where repeatability of measurement with shot-to-shot resolved resolution is of secondary importance, at most, and it is the ensemble average, which is important. These situations are however, outside of the scope of interest of the applicant.

Supercontinuum generation was demonstrated for the first time in 1970 by Alfano and Shapiro in a bulk boron-silicate glass [12], and since then it has started to play increasingly pronounced role in nonlinear optics [13]. The supercontinuum spectrum typically arises from the interaction of a short pulse of an optical pump – for example a mode-locked laser – with the matter of an optical medium. A subtle interaction then takes place between the linear response of the medium, i.e. its chromatic dispersion, and the nonlinear response, especially the $\chi^{(3)}$-type nonlinearity (applicable to glasses and generally to optical materials with inversion symmetry). Optical nonlinearity is manifested by the dependence of the refractive index on the intensity of the incident electric field (the optical Kerr effect). As a result of this dependence, fragments of an optical pulse with different frequencies, experience different delays during propagation. An intensity dependent change of phase, occurring across the pulse frequencies, is referred to as self-phase modulation (SPM). As consequence of SPM, the pulse spectrum broadens. It is possible, that the influence of chromatic dispersion and SPM cancel each other out. An optical wave, propagating in such conditions does not experience change in either the time domain, nor in the frequency domain, and is called the soliton [14]. In physical nonlinear media, such a scenario does not typically take place (without taking specific means). The chromatic dispersion and SPM do not balance each other. What is more, the interaction of linear and nonlinear processes occurs in the form of four-wave mixing (FWM) as well, and the frequency of the pulse is also converted due to Raman scattering. Specifically, the Raman process results in the pulse energy being transferred from the higher frequency components to the lower frequency components. Along with other nonlinear processes, such as soliton fission and self-steeping [15], optical wave breaking (OWB) [16] and dispersive wave emission (DSW, also called Cherenkov radiation) [17], a picture of complex dynamics is formed, and a description of which is nontrivial and mostly impossible to obtain analytically [13]. Numerical methods of nonlinear propagation of an electromagnetic wave in an optical medium have been intensively developed over the recent years [14,18]. Numerical solving of the generalized nonlinear Schroedinger equation (GNLSE), is considered to be the most accurate in reconstruction of the experimental results, under the condition of, sometimes rather difficult, correct parametrization of the nonlinear medium [13].

The choice of the nonlinear medium for supercontinuum generation is of fundamental significance to the properties of the spectral characteristics of the obtained source. The medium of choice for the past two decades has been the optical fiber, and in particular, following its inception – the photonic crystal fiber (microstructured fiber). The arguments supporting this choice are the following:
1) spatial confinement of the radiation in the core area of an optical fiber enables much higher intensities, that in the bulk media, and in consequence it softens the requirement for the pump power necessary to observe the nonlinear effects,
2) photonic crystal fibers allow for the engineering of chromatic dispersion profiles with considerable flexibility; the designing criterion is usually the operational wavelength of the intended pump laser,
3) the radiation is propagated in a form of a guided mode, which enables maintaining of the spatial coherence of the generated supercontinuum spectrum – almost the same as of the pump laser.

The phase coherence of a supercontinuum source is a distinct problem in the area of nonlinear fiber optics research. Existing state-of-the-art draws a clear relation between supercontinuum phase coherence

and the duration of the pump pulse [1]. The sign of the chromatic dispersion profile in the wavelength range covered by the supercontinuum, also has a share of influence over this property [13]. Research work conducted by the applicant with the research group of prof. R. Buczyński at Institute of Electronic Materials Technology, indicated the relation, vastly overlooked in the literature, between the spatial structure of guided radiation and its phase coherence.

Optical pumping with pulses lasting 100 fs or less, centered at a wavelength of anomalous dispersion of the nonlinear medium, typically favors processes of SPM and soliton fission, as well as the solitons' gradual (along the propagation) decrease of frequency due to Raman scattering (soliton self-frequency shift, SSFS). The resulting spectrum maintains high phase coherence in a bandwidth of hundreds of THz [1]. In general, every continuous wave signal with sufficiently high intensity of the electric field experiences break-up into a train of pulses, under the influence of $\chi^{(3)}$ nonlinearity. This effect is called modulation instability (MI) and it is considered the representation of the same physical phenomena as FWM, but in relation to the time and frequency domains, respectively [19]. The 100 fs pulse duration is a conventional figure, above which the MI begins to dominate among the spectral broadening processes. The instability related to the stochastic pulse-to-pulse phase, results from the noise taking part in the process as the seed signal of FWM. The so-called noise-driven supercontinuum sources are usually pumped with pico- and nano-second lasers (e.g. Nd:YAG microlasers) and use nonlinear fibers, which at the laser wavelength have a small value of anomalous dispersion and a positive value of the dispersion slope (dispersion remains anomalous for the longer wavelengths, as well). The combined effects of soliton dynamics, propagation of which is supported in the anomalous dispersion, and of modulation instability, is crucial to the high efficiency, in terms of the spectral width of such sources, despite their phase incoherence [1,13]. In fibers made from unconventional glasses, such an approach enabled supercontinuum generation stretching from around 1 µm up to the mid-infrared around 5 µm (tellurite glass fibers [20] or fluorozirconate, ZBLAN type glass fibers [21]) or even up to 13 µm in multimode fibers made from chalcogenide glasses [22]. The applicant and co-workers have also demonstrated supercontinuum generation under pumping into anomalous dispersion wavelength range of photonic crystal fibers, made of multicomponent soft glasses. The glass used to draw air-glass fiber structures was the in-house developed lead-bismuth-gallate oxide composition [**MK-3,MK-5**]. A tellurium oxide glass was also used for photonic crystal fiber drawing by the applicant and collaborators [**MK-4**].

The symbolic value of pulse duration of 100 fs is not the sole indicator distinguishing between a coherent or incoherent spectral broadening process in a nonlinear optical material. In case of some anomalous dispersion-pumped, octave spanning spectra, considerable drop of coherence has been anticipated numerically for pump pulses as short as 50 fs [1]. The difference comes from the dispersive properties of the fiber and the used pump power. Let's consider characteristic lengthscales in a nonlinear fiber defined as [14]:

$$L_{fiss} = L_D / N \text{, with } L_D = t_0^2 / |\beta_2| \text{ , } N = L_D / L_{NL} \text{ and } L_{NL} = 1/\gamma P_0 \qquad (1)$$

where L_{fiss} − soliton fission characteristic lengthscale, L_D − dispersive char. lengthscale, L_{NL} − nonlinear char. lengthscale, t_0 − time duration of pump pulse (note: time duration of the complex amplitude of pulse, physical duration of pump pulse measured using FROG or autocorrelation, is longer, depending on the pulse shape), β_2 − group velocity dispersion at the pump center wavelength, γ − nonlinear coefficient, P_0 − pump pulse peak power. The physical interpretation of the lengthscales given with formulas (1) is the propagation distances, at which the given phenomenon (soliton fission, dispersive perturbation or nonlinear perturbation) can have an effect on the dynamics of the propagating wave. It is assumed, that the characteristic langthscale, at which the amplification of noise due to modulation instability takes place, is $L_{MI} \sim 16 L_{NL}$ [14]. Another condition for coherent supercontinuum generation can therefore be defined, which refers to the limitation of the order of the input soliton (pump signal), which is N << 16.

In the wavelength range with normal dispersion, where solitons are not supported, modulation instability and related decoherence can also take place [23]. In such a case, the wave mixing process related to MI is seeded by noise (similarly to anomalous dispersion MI), but the pump signals are the spectral components arising from the consecutive orders of Raman scattering. The "threshold" value of the

pump laser's pulse duration for this effect to play a significant role in the spectral broadening, is typically assumed at 200 fs, which is higher, than for anomalous dispersion nonlinear media [2]. Fiber birefringence has also been identified as a possible source of normal dispersion supercontinuum instability [24,25].

Research literature provides different schemes of stabilization of the supercontinuum spectrum. The pumping with tens-of-femtosecond pulses – with the reservations on the length of nonlinear medium related to the characteristic lengthscales and the input soliton order – is the most straightforward solution. When considering the type of supercontinuum for a given application, the technical complexity, size and cost of the pump lasers delivering such short pulses has to be taken into account. Other solutions exist, which take advantage of the interactions between different longitudinal modes propagating in the nonlinear fiber. Apart from the pump laser, a low-power seed signal can also be in-coupled to the fiber (often a continuous-wave signal) at a wavelength corresponding to supercontinuum fragments affected by amplification of noise through the MI. The purpose of the seed signal is delivering spectral components with pulse-to-pulse deterministic phase [26-28]. An alternative way of spectral stabilization is the use of a tapered fiber as the nonlinear medium [29]. In such a fiber, the broadening begins in the part of fiber with anomalous chromatic dispersion at the pump wavelength. The dispersion profile then evolves along the structure towards normal dispersion, before soliton-pumped amplification of noise can take place under the pump conditions intended for such a structure at the design stage. Results of numerical simulations suggest that pulse-to-pulse supercontinuum decoherence can be substantially reduced in just a slightly tapered fiber pumped with self-similarity pre-compressed pulses [30]. This would in turn enable pumping with a relatively simple picosecond laser system. Yet another alternative is containing of the supercontinuum spectrum entirely within the wavelength range, where there is normal dispersion in the nonlinear medium (ANDi – all-normal dispersion). Together with pumping with pulses lasting 200 fs or less, a coherent supercontinuum with a flat spectrum spanning an octave bandwidth has been demonstrated by several research groups in the world [31-34]. In all of these cases silica photonic crystal fibers have been used and the pump wavelength was either 790 nm, 1060 nm or 1560 nm. The only result of ANDi supercontinuum generation in non-oxide glass fibers, to the best of knowledge of the applicant, was reported by authors of [35] (it can be expected, that the development of chalcogenide glass fibers would result in more such demonstrations in the coming years). An innovative all-solid glass fiber was used, which was a hybrid structure made of chalcogenide and fluorozirconate glasses and the supercontinuum spectrum covered wavelengths from 1.2 μm to 2.8 μm. The flatness of the recorded spectrum was however far from satisfactory with a pronounced dip around the pump wavelength (around 2 μm). This problem had been earlier assigned by A. Heidt (University of Bern, earlier ORC Southampton) to the not optimized dispersion characteristic of the nonlinear fiber [36]. In this particular case though it has to be stressed, that dispersion engineering in a pair of these technologically difficult glasses is very challenging. The applicant with collaborators has also studied ANDi supercontinuum generation in photonic crystal fibers with engineered chromatic dispersion and the results of this work are summarized in the following parts of this research statement.

Summary of research results obtained by the applicant
Generation of coherent supercontinuum in photonic crystal fibers with normal dispersion
The first result of ANDi supercontinuum generation in the applicant's group was obtained in 2013 with a spectrum spanning full octave [MK-1]. An all-solid glass photonic crystal fiber was used – its profile of chromatic dispersion and structure layout are shown in Fig. 1. A photonic crystal fiber with an all-solid glass structure has been demonstrated for the first time by Feng et al. [37]. Construction of an all-solid structured fiber requires at least two glasses with different refractive indices, but with thermal properties matched as close as possible. It is especially important to assure similar values of the thermal expansion coefficients and the characteristic temperatures. In the research group, later joined by the applicant, such structures were demonstrated by R. Buczyński and co-workers [38]. Efficient supercontinuum generation in a photonic crystal fiber of this type has not been presented until the first demonstration using an optimized fiber by the applicant and co-workers in the group of R. Buczyński in 2013.
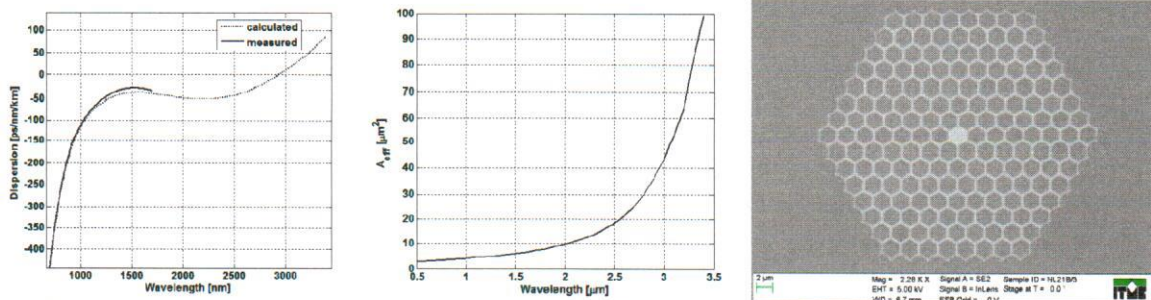
7

Fig. 1. From left to right: chromatic dispersion profile of photonic crystal fiber with all-solid glass lattice designed at ITME, wavelength dependence of the effective mode area and scanning electron microscopy image of a real fiber structure.

The fabricated photonic crystal fiber (Fig. 1) had its core and lattice made of the commercially available F2 glass (Schott). The lattice inclusions were made of boron-silicate glass developed in-house and melted in the Glass Department laboratory at ITME. The composition of this glass labelled NC21A is: (mol.%) SiO_2 - 56.84, B_2O_3 - 23.19, Al_2O_3 - 0.61, Li_2O - 6.23, Na_2O - 9.51, K_2O - 3.63. The refractive indices measured at a wavelength of 1550 nm for the two glasses are n_{F2} = 1.594874 and n_{NC21A} = 1.511304 respectively. Therefore the fiber guides light by total internal reflection. The glass transition temperatures for the two glasses are Tg_{F2} = 569°C and Tg_{NC21A} = 492 °C. Nonlinear refractive indices, measured at 1240 nm [39] are: n_2=2.9 × 10^{-20} m^2/W (F2) and n_2=1.1 × 10^{-20} m^2/W (NC21A). In the work [MK-1] the measurement setup and the optical parametric amplifier (OPA) pump source, made available at the Heriot-Watt University in Edinburgh (UK) was used.

The OPA pump wavelength was set to 1360 nm. The output pulses of this laser system were shorter than 150 fs. The selection of the pump wavelength was motivated by the tuning characteristic of the OPA. This was the longest available wavelength, where the amplifier was still characterized with reasonable efficiency and relatively good spatial properties of the output beam. Additionally, the intent of the applicant's team at this stage was to make use of the wavelength range in which the disposed fiber's effective mode area had been within the limit of 5-7 μm^2. As shown in Fig. 1, the wavelength dependence of the effective mode area over 1800 nm begins a steep upward climb. This translates to a decrease of the nonlinear coefficient according to $\gamma(\omega) = n_2 \cdot n_0 \cdot \omega_0 /c/n_{eff}(\omega)/\sqrt{[A_{eff}(\omega) \cdot A_{eff}(\omega_0)]}$, which is approximately $\gamma \sim A_{eff}^{-2}$, i.e. the nonlinear coefficient drops with the increase of a square of the effective mode area. The result of supercontinuum generation experiment in these conditions was a spectrum covering wavelengths from 900 nm to 1900 nm, which corresponds to an octave. The recorded spectrum and its numerical reconstruction, are shown in Fig. 2. The shape of the measured spectrum and specifically its short-wavelength and long-wavelength edges were reconstructed in the simulation very accurately. It can be observed in Fig. 2, that a prominent spectral feature around the pump center wavelength, present in the measured spectrum, was not reproduced by the numerical model. This feature is related to the part of pump light being coupled into the photonic lattice (photonic cladding) of the fiber. This area in the fiber has the refractive index higher than the tube surrounding the microstructure containing the lattice and the core. Because of this, the photonic lattice supports index guiding. The consequences of this are discussed in detail in a following part of the research statement. In the work [MK-1] the applicant conducted analysis and discussion of the experimental results, prepared the numerical model (propagation of radiation in the fiber modelled with the GNLSE) taking into account the frequency dependence of the effective mode area, and performed numerical simulation of nonlinear propagation, and finally compared the experimental and theoretical results of supercontinuum generation. This was the first demonstration of an octave-spanning ANDi supercontinuum generation in an all-solid glass photonic crystal fiber.
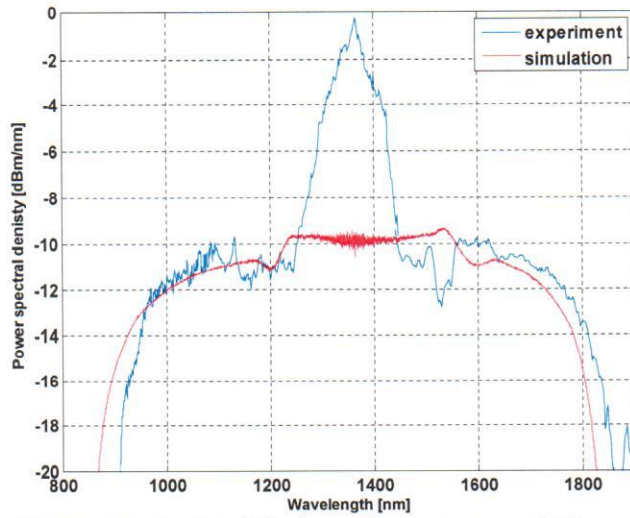
8

Fig. 2. Supercontinuum generation in all-solid glass photonic crystal fiber of the NL21 series, optical pumping with 150 fs pulses, measurement result and numerical simulation.

In the research paper which followed, the applicant's team designed and fabricated a series of all-solid glass photonic crystal fibers in a family designated "NL21", [**MK-2**]. The structure of these fibers is similar to the one shown in Fig. 1. Through the change of geometrical parameters, such as the diameters of the core and the photonic cladding, the pitch and relative inclusion size, the team designed a family of fibers with chromatic dispersion shown in Fig. 3. The geometrical parameters of the fibers in the series are listed in Table 1.
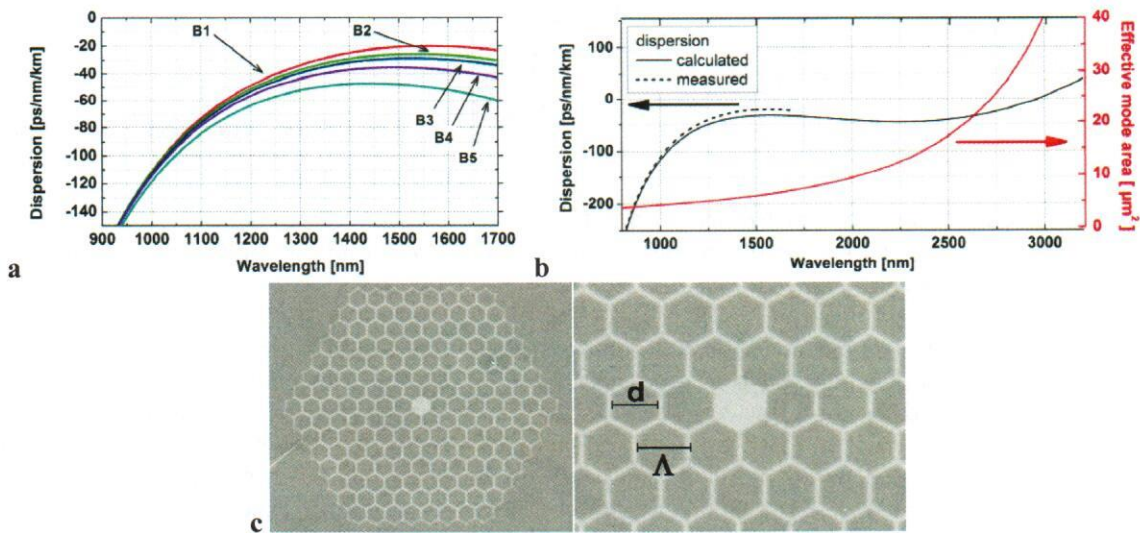

Fig. 3. a: Measured chromatic dispersion profiles of the fabricated fibers, b: the dispersion profile (measured and theoretical) and the wavelength dependence of the effective mode area of the fiber in which the broadest supercontinuum spectrum was recorded, c: SEM images of this particular fiber (dimension symbols correspond with Tab. 1).

9

Table 1. Geometrical parameters of the series of all-solid glass photonic crystal fibers with all-normal dispersion, as used in the paper [MK-2].

no.	outer diam. (µm)	lattice diagonal (µm)	width of the core (µm)	inclusion diam. (µm)	d/Λ (−)
B1	143.0	35.61	2.43	2.15	0.91
B2	140.3	35.06	2.40	2.13	0.91
B3	136.6	34.65	2.37	2.11	0.91
B4	131.0	33.33	2.25	1.99	0.91
B5	128.8	31.55	2.13	1.93	0.91

The fabricated fibers have almost flat dispersion profiles in a wide range of wavelengths. The change of the lattice geometrical parameters (decrease of overall lattice size) results in the change (increment) of the absolute value of dispersion of the flattened section of the dispersion profile, as well as a red-shifting of its local maximum. Detailed studies of these dependencies were reported by R. Buczyński and T. Martynkien [40]. The family of supercontinuum spectra, recorded in the fabricated fibers under pumping with 70 fs pulses centered at 1550 nm, is shown in Fig. 4a. The pump source in these experiments was an OPA setup at the laboratory of prof. Czesław Radzewicz at the Institute of Chemical Physics, Polish Academy of Sciences, where the experimental part of work took place. In the best case (fiber B1 as listed in Tab. 1) the spectrum spanned a wavelength range from 900 nm to 2300 nm. At the time of publication of this result in Optics Express, this was the broadest supercontinuum spectrum in an ANDi fiber pumped at a typical erbium laser wavelength (around 1550 nm).
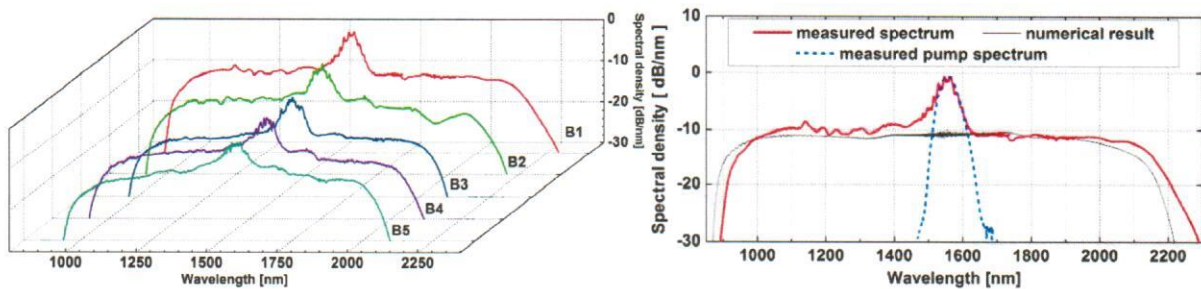

Fig. 4. a: Supercontinuum spectra recorded for the ANDi fibers listed in Tab. 1., measured under pumping with 70 fs centered at 1550 nm, b: the broadest recorded spectrum in the NL21B1 fiber, its numerical reconstruction with a GNLSE model and measured pump laser spectrum.

In the paper [MK-2] the applicant conducted numerical simulations with his nonlinear modelling tools based on GNLSE, followed by analysis and discussion of all experimental and numerical results. In conclusions to this discussion, the applicant identified the physical processes behind the spectral broadening. The applicant noted, that rigorously parametrized GNLSE model for the discussed case (time duration and energy of the pump pulse, its temporal envelope, chromatic dispersion and wavelength dependence of A_{eff} in the fiber) enables precise numerical reconstruction of experimental results, which facilitates identification of the constituents of the broadening dynamics. The comparison of experimental and numerical data is shown in Fig. 4b. The discrepancy between experiment and simulation can be clearly noted, but it is contained to wavelengths around the pump wavelength. The prominent spectral feature was assigned to a part of pump pulse energy coupled with each laser shot into the photonic cladding. This part of pump pulse energy is then propagated in the lattice and does not participate in the nonlinear broadening process. The nonlinear process itself comprises several physical phenomena. Their sequence, described by the applicant for the case of ANDi fibers designed at ITME, had been discussed earlier, as well, e.g. by the authors of paper [36]. The entire process can occur fast over typical nonlinear fiber lengths, as shown in Fig. 5a. At the initial stage, the spectrum broadens due to SPM – it is manifested

by the characteristic "S" shape of the time-wavelength profile (spectrogram, Fig. 5b – numerical result). The next phase begins with modulation at the leading and trailing edges of the propagating supercontinuum pulse (in time domain), which is generally assigned to the effect of OWB. In the spectral domain this corresponds to the beating between the new OWB features and the parts of spectrum where OWB is yet to occur (or the other way, depending on the direction of wavelength shifting) – Fig. 5c. In the frequency domain, a mixing effect takes place between the SPM components and the OWB components, which leads to onset of the parametric sidebands of the spectrum – Fig. 5d.
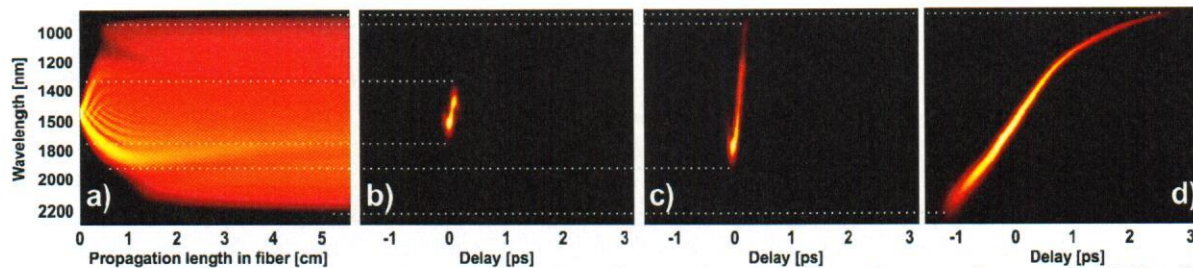

Fig. 5. *The sequence of physical processes broadening the ultrashort laser pulse in an ANDi fiber, a: evolution of the spectrum along the entire nonlinear fiber length, b: SPM-dominated phase, c: OWB at the leading and trailing edges of the pulse, d: onset of parametric sidebands.*

Notably, the ANDi nonlinear process described above, occurs fast, that is over the initial centimeters of the fiber length. Analysis of the numerical simulations based on GNLSE enables to conclude, that this stems from the optimal design of the fiber's dispersion profile. Specifically, this is achieved by such a selection of the geometrical parameters of the photonic lattice, that there is a proper balance between the linear effects (dispersion) and the nonlinear effects, here namely SPM and FWM. The short propagation length, over which the spectrum is formed, has tremendous meaning to photonic crystal fibers drawn from soft glasses (and oxide soft glasses in particular), as these fibers usually suffer from larger attenuation, compared to e.g. silica or fluoride fibers. Attenuation of the NL21 series fibers is at the level of 2-3 dB/m. The discussed process occurring under pumping such as the one used in the works [MK-1,MK-2] is coherent, in a sense, that it is phase-preserving shot-to-shot. This is because the SPM and OWB processes are intrinsically self-seeded. The 70 fs pump pulse duration is short enough, so that the Raman response of the fiber glass, which is delayed against the Kerr nonlinearity response, does not influence significantly the spectral broadening in the perspective of the pump pulse duration. In the course of his research, the applicant studied and identified the role of delayed Raman scattering, and the role of the part of the pump pulse energy propagating in the photonic lattice, in the shaping of the coherence properties of ANDi supercontinuum under pumping with 400 fs long pulses.

Results reported in the works [MK-1,MK-2] were obtained by the applicant and team in the fibers made from silicate glasses. Selected glasses of this type allow for joint thermal processing, i.e. fiber drawing at a drawing tower, because their rheological properties are very similar. The research in this area was conducted by the team at the Glass Department, ITME, including research in which the applicant took part [41]. Silicate glasses have transmission window, which is limited by multiphonon absorption for wavelengths longer than 2.6-2.7 μm. This precludes the use of these materials in designing of ANDi fibers for coherent supercontinuum generation in the very attractive range of wavelengths in the mid-infrared. Another limiting factor are the relatively low values of nonlinear refractive index, which translates to lower efficiency of supercontinuum generation, or straightforwardly excludes supercontinuum generation entirely, due to the typical attenuation level of silicate glass fibers. Practice shows, that it is usually an order of magnitude higher, than in step-index or photonic crystal fibers drawn from the silica glass. The solution proposed at the group of the applicant was based on the development of the synthesis of multicomponent glasses composed of heavy metal oxides. This type of glasses feature high values of the nonlinear refractive index (one-two orders of magnitude higher than silicate or silica glass fibers) and their transmission window extends to 5 μm. These glasses hence can be considered an attractive

alternative to the non-oxide chalcogenide glasses, due to much simpler technology and better chemical and mechanical properties. Moreover, multicomponent heavy metal oxide glasses developed at ITME have transmission windows starting at the visible wavelengths (roughly 500 nm), which enables designing of photonic crystal fibers for supercontinuum generation in the visible, near-infrared and mid-infrared. This is impossible with chalcogenide glasses, since their transmission starts at around 1 μm. Nevertheless, heavy metal oxide soft glasses share the decreased laser damage threshold with their chalcogenide counterparts.

Development of photonic crystal fibers from alternative nonlinear glasses for the mid-infrared range

Research for the alternatives to the silica fibers discussed above focused at the applicant's team at ITME on two types of glasses: a lead-bizmuth-gallate oxide glass with the chemical composition of $40SiO_2$, $30PbO$, $10Bi_2O_3$, $13Ga_2O_3$, $7CdO$, designated PBG08, and on a tellurite glass with the composition $65TeO_2$ $28WO_3$ $7(Na_2O+Nb_2O_5)$, designated TWPN/I/6. Each of these compositions was used, with success, for photonic crystal fiber drawing. At the present stage of research work, the lack of a thermally matched composition with sufficiently different refractive index value, did not allow to fabricate all-solid glass photonic crystal fibers with these new materials. Both types of the developed fibers had therefore a solid glass core and a regular, hexagonal photonic lattice composed of air holes. Chromatic dispersion profiles and SEM images of fiber structures are shown in Fig. 6. The PBG08 glass fiber was designated "NL24", and the TWPN/I/6 glass fiber – "NL20". The air-glass structure imposed some limitations on the dispersion design flexibility, compared to an all-solid glass approach. For this reason, none of these fibers enabled efficient ANDi supercontinuum generation. The dispersion profiles of the fibers had a zero dispersion wavelength of about 1500 nm and were hence designed with the intent of efficient generation of a solitonic supercontinuum. The supercontinuum spectra, generated in these fibers with pump pulses centered at 1550-1560 nm covered wavelengths between 900 nm and 2700 nm. Typical spectra are shown in Fig. 7. The results were published in the works [MK-3,MK-4].
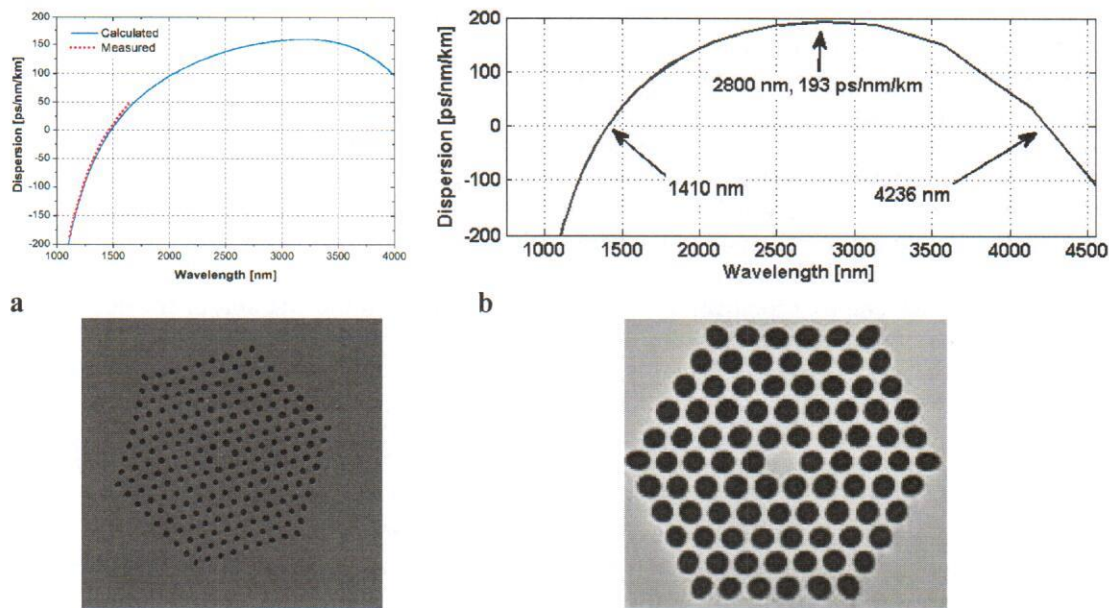

Fig. 6. Chromatic dispersion characteristics and SEM images of real fiber structures of the photonic crystal fiber series a: NL24 and b: NL20.
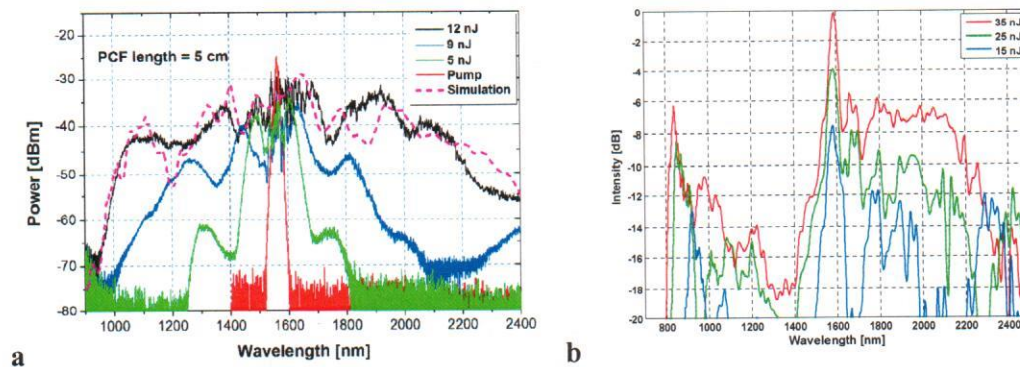
Fig. 7. Supercontinuum spectra in fibers of the NL24 (a) and NL20 (b) series, recorded for pumping into the anomalous dispersion wavelengths of fiber. [MK-3,MK-4]

At the core of achievement in both papers is the demonstration of successful technological attempt to fabricate photonic crystal fibers using the two heavy metal oxide soft glasses, as well as demonstration of the feasibility to obtain an octave spanning spectrum in both fibers. In the paper [MK-3] the applicant and team reported on the fiber with a complex microstructure, in which the lattice contained rings of air holes with different diameters. The innermost ring with the largest diameter of air holes assures propagation of the fundamental mode in the core. Changing of the air hole diameter in the second innermost ring and in the remaining, outer rings for once allowed to control the chromatic dispersion profile and for limiting the waveguide losses of exclusively the fundamental mode. Lower diameter of the lattice air holes in the remaining rings was introducing loss to the propagation of higher order modes. It is difficult to maintain the geometrical parameters, especially the uniformity of the difference of air hole diameters, between the first and the other rings, in a structure like this. Therefore demonstration of a real, fabricated fiber stands for the value of this work. The other important point and scientific value in the paper [MK-3] was the demonstration of supercontinuum generation under pumping from a fiber based, erbium laser. The laser delivered mode-locked pulses lasting 400 fs or almost 1 ps, depending on the mode-locking scheme used. The laser consisted of a seeding oscillator and a chirped pulse amplification block (CPA, [42]). The average output power was relatively high at single watts level and the supercontinuum average output power was reaching 1 W. This is an important achievement, considering the nature of glass used for fabrication of the nonlinear fiber and its laser damage threshold, much lower than the commercial nonlinear fibers made from the silica glass. The pumping laser used in these experiments was designed and built by the members of the Laser and Fiber Electronics Group of prof. Krzysztof M. Abramski from Wroclaw University of Technology.

The fiber reported in the paper [MK-4] was pumped from an OPA source, which generated 120-150 fs pulses, tuned to 1550 nm. In this case the novelty was within the first demonstration of an octave spanning supercontinuum-capable, nonlinear photonic crystal fiber, which was made from a tellurite glass and had a regular, hexagonal lattice of air holes. All earlier literature reports described nonlinear tellurite glass fibers designed in the suspended core fashion, where the core area runs along a large hole in the middle of the fiber structure, supported by typically three thin struts. The large refractive index contrast between the core and the cladding – which consisted mainly of air – is an advantage providing good mode confinement and improving nonlinearity. On the other hand, the dispersion profile in such a fiber is extremely sensitive to geometrical imperfections of the structure. A regular lattice fiber allows larger tolerance in the dispersion profile engineering, but in the case of soft glasses, it is technologically more challenging. The reason is that a regular lattice structure usually requires more thermal processes (drawing), compared to the suspended core fibers. Increased number of thermal processes (i.e. drawing runs) increases the risk of glass recrystallization, which is a source of significant fiber loss or simply does not allow to draw a fiber at all (due to poor mechanical properties). The demonstration of a regular lattice photonic crystal

fiber, made of this type of glass, was therefore an important step forward in the technology of nonlinear glass and microstructured fiber with transmission window extending into the mid-infrared. It required mastering of the glass synthesis and fiber drawing such, as to eliminate recrystallization at every step of the technological process.

In the part of the applicant's research devoted to the development of new nonlinear photonic crystal fibers, there is also the paper [MK-5], in which the applicant's team developed and characterized nonlinear properties of suspended core fibers. The fiber fabricated and reported in [MK-5] was made from the PBG-08 glass. The study revealed however, that it did not have satisfactory linear characteristics. Despite this, the obtained result was an important contribution to further research on this type of fiber structures, conducted in the applicant's research group. It turns out, through numerical simulations, that a properly arranged proportions of the structure designed with the PBG-08 glass, can potentially yield all-normal dispersion profiles with a broad, flattened section of the characteristic, making it suitable for pumping with erbium (about 1.56 μm) or thulium (about 1.9 μm) laser wavelengths.

The contribution of the applicant in the works [MK-3,…,MK-5] was the preparation of numerical models and modelling, participation in the technological processes of photonic crystal fiber drawing, analysis of all experimental and numerical results and the discussion. An important aspect of all these works for the applicant was building of the immediate research environment, including all numerical analysis tools, as well as establishing lasting connections with other research groups. The key in this context was the relation with the Laser and Fiber Electronics group of prof. K. M. Abramski from Wrocław University of Technology, in cooperation with whom the applicant achieved some of the most important results of the presented statement.

New methods of enhancement of the coherence properties of supercontinuum generation

Application of the sub-picosecond laser from prof. Abramski's group to pump the ANDi NL21 type fibers did not seem attractive at first. Existing state of the art confirms, that with pump pulse durations exceeding 200 fs, the coherent ANDi spectral broadening would be distorted by spontaneous Raman scattering [2]. Since Raman scattering in such a situation is usually accompanied by FWM [18], even with solitons not supported, the energy is rapidly transferred to the anti-Stokes and Stokes Raman bands of the pump wavelength, and these new components act as pumps in a noise-seeded FWM. Thus noise is amplified even when the nonlinear medium has only normal dispersion, and this is in fact analogic to the MI with the solitons acting as pump in anomalous dispersion.

Motivated mainly by the intent to explore the laser damage threshold of the NL21 series ANDi fibers under energetic pumping with CPA erbium fiber-based laser, the applicant conducted such an experiment. The clearly better stability of the spectrum of supercontinuum generated in the NL21 fibers, compared to the anomalous dispersion NL24 series fibers, observable even in averaging optical spectrum analyzer measurements, was stimulating scientific curiosity. Research, which followed on the investigation of the phase coherence and the spectral coherence of supercontinuum generation in these conditions, resulted in the two papers [MK-6,MK-7]. The work was conducted in cooperation with dr Grzegorz Soboń and prof. Krzysztof M Abramski from Wrocław University of Technology. All experiments involved an erbium fiber-based CPA pump laser system. The individual pump pulses lasted about 400 fs and the center wavelength was 1560 nm, pump pulse repetition rate was 40 MHz. The goal of work was the characterization of the phase coherence and spectral stability, as well as spectral correlation in supercontinuum generation, using the NL21 series ANDi fibers. Anomalous dispersion fibers of the NL24 series were also used in the work with the correct assumption, that the supercontinuum dynamics in these fibers would be easy to anticipate (in a sense, that the spectrum would be incoherent) and consistent with the state of the art. The NL24 fiber was therefore intended as a validator of the taken research methodology.

The phase coherence, that is phase fluctuation of the spectrum, occurring from shot-to-shot, was investigated with a standard Michelson type interferometer with unequal path lengths. Fluctuations of the spectral intensity from shot-to-shot were resolved with the dispersive Fourier transformation method (DFT, [43-45]). Carefully selected dispersive medium, for example a single mode fiber, a pair of

diffraction gratings or prisms, can be used to stretch an optical pulse in the time domain. With simultaneous limitation of the pulse energy delivered to the stretcher element, it is possible to avoid its nonlinear response and the pulse spectrum remains unchanged. The chromatic dispersion of the stretcher element should not change sign within the wavelength range covered by the spectrum being resolved. If these conditions are met, then the temporal envelope of the stretched pulse maps into its spectrum. In order to investigate the spectral fluctuations of the supercontinuum, the applicant designed a DFT measurement setup, according to the described scheme. The setup was later realized by dr. Grzegorz Soboń from the Laser and Fiber Electronics Group at Wrocław University of Technology. The setup and the idea of the DFT measurements are shown in Fig. 8.

The main components of the used setup are: the dispersive medium – 1 m or 3 m (depending on supercontinuum spectral width) of DCF-38 fiber with normal dispersion up to about 1900 nm, a fast photodiode with 20 GHz bandwidth and a fast oscilloscope with 13 GHz bandwidth. The result of the measurement is an oscillogram showing temporal envelopes of the consecutive pulses. With maintained linear conditions of stretching in the dispersive element (no nonlinear perturbation of the spectrum of pulses), the frequency scale (and thus the wavelength scale) is obtained from the oscilloscope time-base according to formula (2) [44-45]:

$$T(\omega) = \sum_{m=1}^{\infty} \frac{\beta_{m+1} \cdot z}{m!} \cdot (\omega - \omega_0)^m \qquad (2).$$

Using this scheme, the applicant and collaborators realized the time-resolved measurements of the output pulse spectra of the pump laser (400 fs) and of the supercontinuum (typically several ps up to 20 ps, based on numerical estimations).
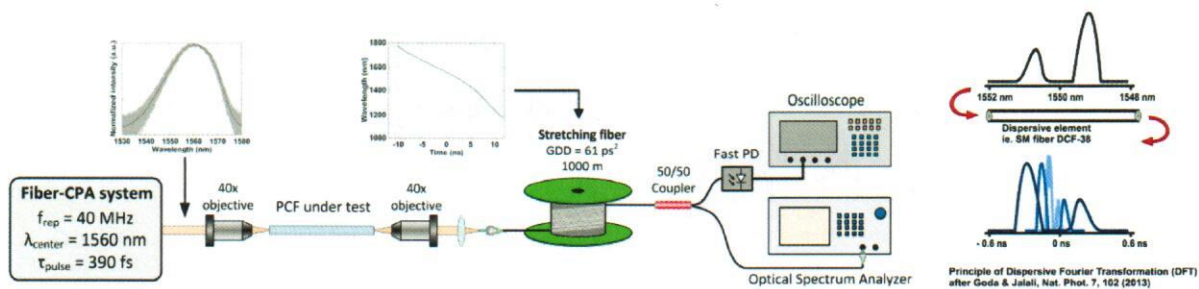

*Fig. 8. Measurement setup and idea of operation of the dispersive Fourier transformation method for measurement of spectra fluctuation of ultra-fast radiation pules [**MK-6**].*

The measurement allowed for linear stretching of pulses originally much shorter than the rise and fall times of available detectors (for the photodiode used in the experiments it was about 140 ps), up to about 10 ns. The length of the dispersion medium, where the investigated pulse is stretched, has to be selected such, that the total introduced group delay allowed maintaining of a satisfactory resolution of the spectrum retrieved from the oscillogram on one hand. The upper limit on the stretching is imposed by the overlapping of consecutive pulses, which obviously cannot take place. In the discussed case, the upper limit was set by the repetition rate of the pump lasers, which was 40 MHz, corresponding to 25 ns. It is to be noted, that a DFT measurement losses phase information and only the measurement of the pulse spectrum is possible. This motivated simultaneous measurements of the interference of the generated supercontinuum pulses to assess their phase coherence, as well.

Results of measurements of supercontinuum pulse interference for the NL24 (anomalous dispersion) and NL21 (ANDi) series fibers are shown in Fig. 9 for different pump powers. The modulus of complex degree of coherence, carrying the information on the pulse-to-pulse phase variability across a wavelength range is mathematically defined as:

$$\left| g_{12}^{(1)} \left(\lambda, t_1 - t_2 = 0 \right) \right| = \left| \frac{\left\langle E_1^* \left(\lambda, t_1 \right) E_2 \left(\lambda, t_2 \right) \right\rangle}{\left[\left\langle \left| E_1 \left(\lambda, t_1 \right) \right|^2 \right\rangle \left\langle \left| E_2 \left(\lambda, t_2 \right) \right|^2 \right\rangle \right]^{1/2}} \right| \qquad (3)$$

In case of experimental data, the coherence degree is simply the interference fringe contrast. The pump conditions in all phase coherence measurements (Michelson type interferometer) were the same – erbium fiber laser with CPA, $\lambda_0 = 1560$ nm, $\tau_0 = 400$ fs. The supercontinuum pumped into anomalous dispersion (NL24 fiber) reveals phase coherence properties consistent with expectations. For the smaller input pulse energy (Fig. 9a) over a fixed length of fiber the characteristic lengthscales for nonlinearity and for the MI are favorable for the SPM and soliton fission, rather than for noise amplification. For the larger pump pulse energy this situation is reversed and noise can be amplified earlier over the fiber sample length, hence the supercontinuum experiences decoherence (Fig. 9b). This type of dynamics of anomalous dispersion-pumped supercontinuum is consistent with existing state of the art [1].
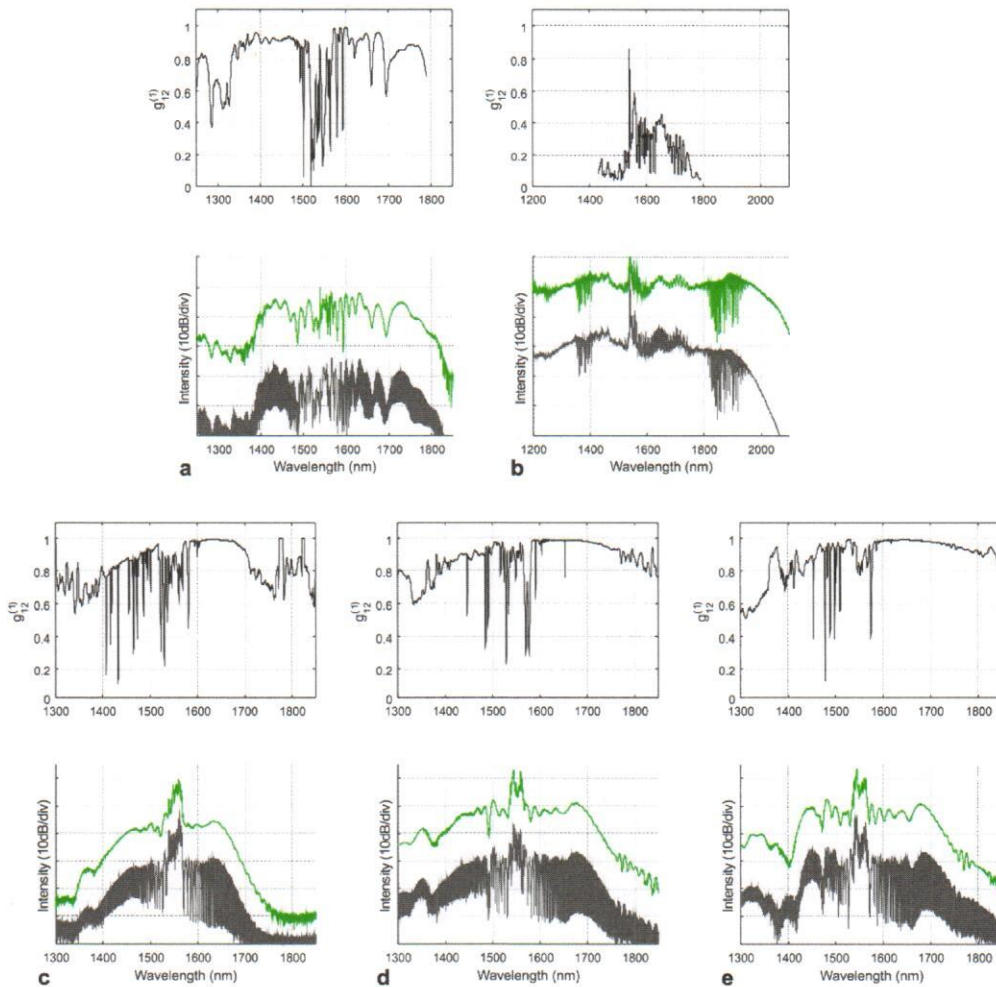

Fig. 9. *Results of interference measurements of SC spectra and profiles of spectral degree of coherence: a) anomalous dispersion-pumped PCF, coupled pump pulse energy $E_{in} = 2$ nJ, b) anomalous dispersion-pumped PCF, $E_{in} = 5$ nJ, c) ANDi PCF, $E_{in} = 2$ nJ, d) ANDi PCF, $E_{in} = 3$ nJ, e) ADNi PCF, $E_{in} = 5$ nJ.* [**MK-7**]

Results of phase coherence measurements for the ANDi fibers of the NL21 type are surprising. The applicant expected rapid decoherence, as soon as the sidebands of spectrum begun to appear, outside of the band dominated by SPM. In case of the NL21 type ANDi fibers, this is a spectrum broader than 1400-1650 nm. It turned out however, that despite the pulse duration long enough to allow Raman scattering in the broadening process, the supercontinuum spectrum maintained phase coherence even when the pump pulse energy was increased – Fig. 9c,d,e. This is in contrast with the state-of-the-art, since it has been shown, that Raman scattering disrupts the generation of coherent side bands in an OWB-parametric process, in such a way, that the parametric process occurs with the noise as seed and the Raman components as the pump signals [2].

The second part of research published in [**MK-6,MK-7**] was devoted to the spectral coherence, which is related to the shot-to-shot intensity fluctuation of the spectrum of supercontinuum. The measurements, done using the DFT method, returned ensembles of over 1200 spectra of consecutive supercontinuum pulses recorded for the NL24 and NL21 fibers. Fig. 10 shows the dramatic difference in the stability of spectrum shot-to-shot. For the NL24 fiber, the fluctuation of spectrum does not drop below 7 dB, except for the wavelengths immediately next to the pump. The ANDi spectrum in NL21 fiber also fluctuates, but the amplitude of these variations is significantly smaller and in almost the entire investigated spectral range it remains within 1 dB. It is interesting to note the shape of the signal-to-noise ratio profiles (SNR) for both fibers (Fig. 10), which here is the measure of the shot-to-shot spectral fluctuation. Firstly, the SNR for both fibers is similar around the pump wavelength. In the NL24 fiber it does not improve with the detuning from the pump. In the ANDi fiber of the NL21 family, on the contrary, the noise is quenched as the spectral side bands develop. Moreover, the profile of SNR in the NL21 fiber supercontinuum has a characteristic train of local maxima extending towards the shorter and longer wavelengths from the pump. For an in-depth analysis of these interesting phenomena, the applicant used spectral correlation analysis to peek into the relative dynamics among individual spectral components of the generated supercontinuum spectra. Spectral correlation analysis of supercontinuum has recently been proposed by the group of prof. John Dudley from Universite de Franche-Comte in Besançon, France [44,45]. The correlation in this approach is discussed using a map, calculated according to formula (4):

$$\rho(\lambda_1, \lambda_2) = \left| \frac{\langle I(\lambda_1)I(\lambda_2)\rangle - \langle I(\lambda_1)\rangle\langle I(\lambda_2)\rangle}{\sqrt{\left(\langle I^2(\lambda_1)\rangle - \langle I(\lambda_1)\rangle^2\right)\left(\langle I^2(\lambda_2)\rangle - \langle I(\lambda_2)\rangle^2\right)}} \right| \tag{4}$$
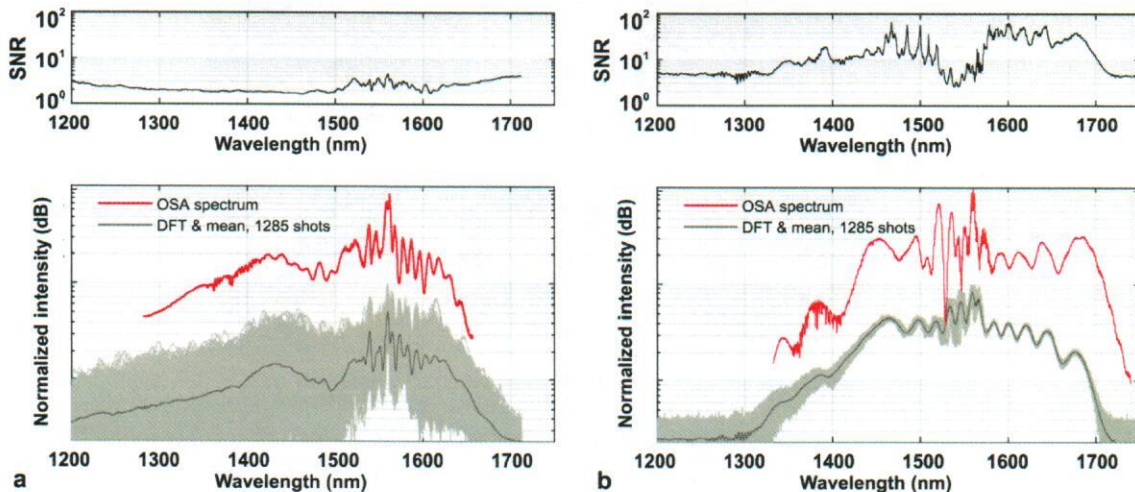

Fig.10. The SNR and the ensembles of single-shot spectra obtained using DFT and averaged spectra recorded with an OSA before the stretching fiber for the investigated soft glass fibers : a) anomalous dispersion pumped NL24 fiber and b) all-solid, all-normal dispersion NL21 fiber.

The map contains values from -1 to 1. The Cartesian coordinates of the map represent each possible pair of wavelengths in the supercontinuum. The value of 1 stands for full correlation, that is when the intensity at both correlated wavelengths either increases or decreases at a given time. The value of -1 represents a situation when the two wavelengths are anti-correlated. When the intensity at one of them increases, then at the other one the intensity decreases. The diagonal from the lower-left corner to the upper-right corner contains values of 1, which is a trivial confirmation of every wavelength being at full correlation with itself. The map is also symmetric against this diagonal. Spectral correlation maps (or simpler "correlation maps") often enable to observe in the supercontinuum dynamics the subtleties otherwise impossible to record in ensemble averaging or even in the averaging measurements retaining the phase information [44]. The correlation maps calculated according to formula (4) using the experimental data for the NL24 and NL21 fibers, are shown in Fig. 11.
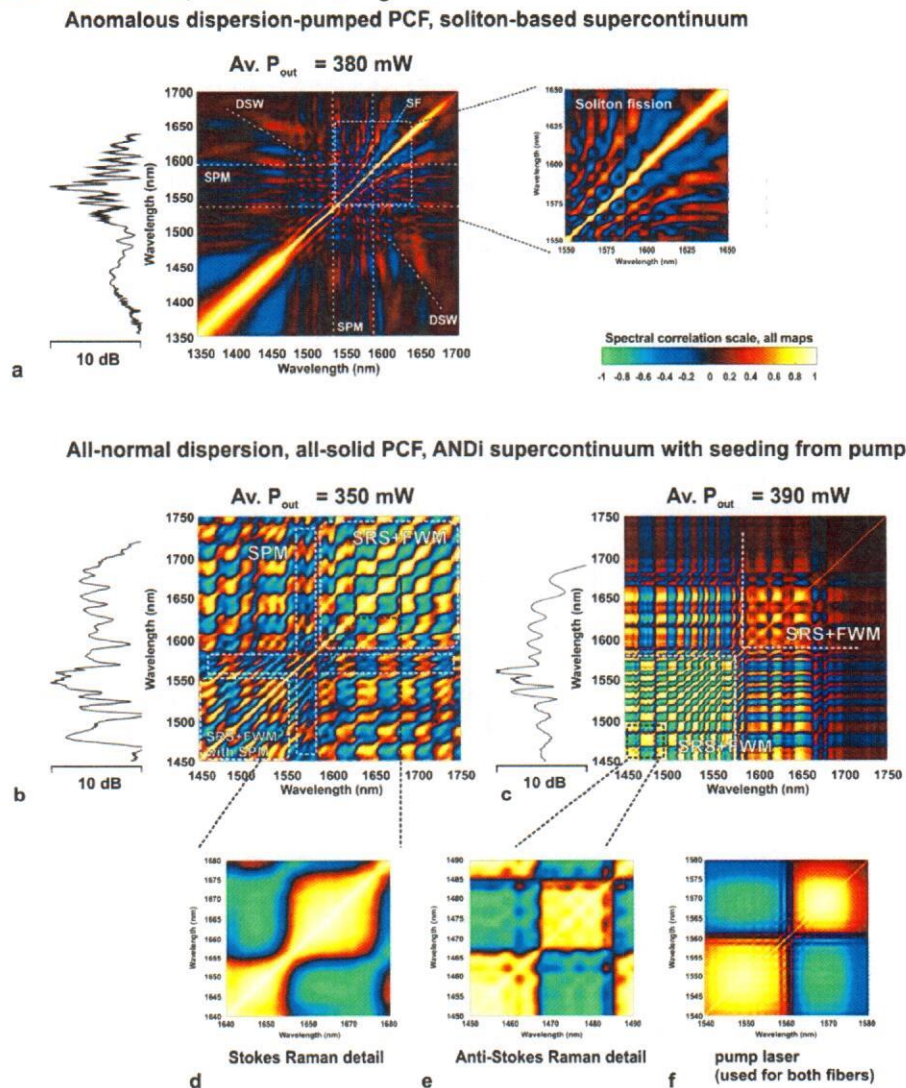

Fig. 11. Spectral correlation maps obtained with DFT for investigated soft glass fibers. Typical features of self-phase modulation (SPM), soliton fission (SF) and calculated location of the dispersive wave (DSW) are indicated for the soliton-based supercontinuum. ANDi supercontinuum correlation is shown indicating formation of pump-seeded Raman components, first at Stokes-shifted wavelengths (lower in-coupled pump power), followed by anti-Stokes shifted wavelengths (higher in-coupled pump power), SRS – stimulated Raman scattering, FWM – four-wave mixing. Spectral correlation of the pump laser line is shown in the bottom-right. [**MK-7**]

The correlation map obtained from experimental data for the NL24 fiber (pumping into anomalous dispersion) – Fig. 11a – contains traces typical to soliton dynamics and within the pump pulse energy range, when the MI does not yet dominate over the other effects. These are SPM, soliton fission (SF) – here the characteristic bending of the correlated spots towards the longer wavelengths is an expression of SSFS, finally DSW is also observable. Two correlation maps were calculated for the NL21 fiber and the ANDi supercontinuum generation. The process of spectral formation, shown in Fig. 11b,c, can be divided into two phases, separated with a certain pump power threshold (average pump power between 350 mW and 390 mW). The characteristic feature of both maps is the presence of a jitter-like pattern [44]. When the pump power is below the mentioned threshold – Fig. 11b – this pattern can be observed at the red-shifted wavelengths of the spectrum [**MK-6**], while over the threshold, it appears at the blue-shifted side of spectrum. In both cases the applicant assigned these "foot-prints" to the interaction of FWM and Raman scattering [14]. The existence of a certain pump power threshold in the correlation pattern dynamics supports this assignment, because the anti-Stokes wing of Raman scattering signal is usually 1-2 orders of magnitude less intense, than the Stokes-shifted wing. The accompanying process of FWM, in which the following orders of Raman scattering of the initial pulse (i.e. the pump pulse) are the FWM pump signals, makes the anti-Stokes Raman wing strong enough, so it is only roughly 20-30% below the level of the Stokes-shifted wing. This is also why there is a relatively low separation between the values of "below-threshold" and "above-threshold" pump powers observed in the experiment for this process (the applicant uses the "threshold" term rather symbolically, since observation of strictly threshold-like dynamics here is not of the essence to the discussed problem). According to the existing state of the art, ANDi supercontinuum generation dominated by Raman scattering should be both phase- and intensity-incoherent, because the Raman component-pumped FWM process then amplifies the noise [2]. The phase coherence measurements of supercontinuum obtained in the ANDi NL21 fiber are however in contrast to this. An explanation was proposed by the applicant, after measuring the spectral correlation pattern of the pump laser, which was used in the DFT measurements. The obtained correlation map is shown in Fig. 11f. Comparing this pattern with the traces present in the long-wavelength and short-wavelength sides of the ANDi spectrum (Fig. 11d,e) suggests the direct contribution of the pump laser in the supercontinuum dynamics. This conclusion may seem trivial, because the pumping laser is the source of energy for the supercontinuum and it is this laser's spectrum, which is broadened. Nevertheless, the correlation map of the laser, shown in Fig. 11f, was calculated for the laser beam before its coupling into the nonlinear fiber, while the ANDi supercontinuum correlation maps were calculated obviously from the data recorded at the output of the nonlinear fiber. It is to be noted, that the structure of the NL21 fiber enables propagation of light in the photonic lattice, not only in the core. In fact, this is similar to the double clad fibers known from the fiber laser technology. From the point of view of nonlinear optics, it is important to distinguish between the core of the NL21 fiber and its photonic lattice (photonic cladding) with respect to the nonlinear response of the two areas. In the core, the nonlinear processes are supported by strong spatial confinement, that is by a small effective mode area (the typical fiber of the NL21 family has a core diameter of 2.5-3.0 μm, depending on particular type), while the photonic lattice has a diameter of 35 μm (the diameter taken as the circle diameter inside the hexagonal area of lattice). Hence the nonlinear response of the lattice can be safely considered negligible. This allows to assume that the radiation in the lattice is propagated only in a dispersive manner and no nonlinear phase distortion of the pump light takes place. Such assumption is further supported by linear simulations, which reveal that the lattice supports multiple higher order modes. The electric field of these modes is distributed with different patterns across the lattice, but usually away from the nonlinear core. Still, their overlap with the fundamental mode in the core is non-negligible. Results of these simulations in the form of selected modes distributions – of the fundamental mode in the core and three higher order modes from the photonic cladding – are shown in Fig. 12.
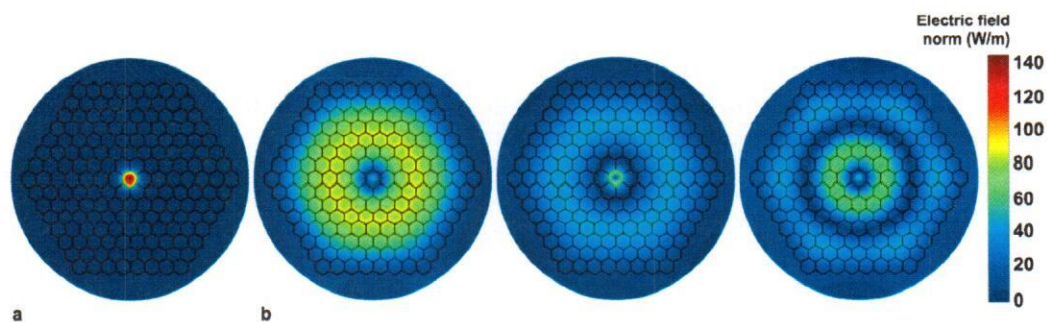
Fig. 12. Mode field distributions – a: fundamental mode in the core and b: selected higher order modes in the photonic cladding of the NL21 type ANDi fiber. Results of modelling with the finite element method.

During the in-coupling of the pump laser radiation into the core of the NL21 series fibers, a part of the energy excites higher order modes in the lattice. The propagation of these modes in the lattice and not in the core of the fiber, has substantial consequences to the coherence properties. In the case, where the pump pulse is short enough, so that Raman scattering does not influence the broadening significantly, the role of the cladding modes is indeed elusive, since the supercontinuum is coherent by the nature of the involved self-seeded processes (SPM, OWB). Dramatically different situation takes place, when the pulse is long enough to allow Raman scattering dominate over OWB. As a remainder: according to literature it is about 200 fs [2], in the applicant's experiment the pump pulse lasted almost 400 fs, the precise "threshold" value for the Raman scattering domination in broadening depends on the Raman temporal response curve of the fiber glass. The applicant was the first to observe and to suggest, that in these conditions the nonlinearly undisturbed pump laser light (only dispersively stretched) propagated by the lattice around the nonlinear core, delivers to the core – through mode coupling – a spectral component with a deterministic phase. Deterministic for this instance means invariable from pulse to pulse. The deterministic phase component at every step of propagation is the seed signal for the four wave mixing process, pumped by the Raman components, arising from Raman scattering, during the spectral broadening process in the fiber core. The deterministic signal (maintaining its phase pulse-to-pulse) therefore substitutes the noise components. The amplification of noise is surpassed and the spectrum remains coherent. An alternative hypothesis is a scenario, in which the noise is not amplified simply because a part of the pump power leaks into the cladding – the energy in the core drops and the spectrum remains coherent, analogically to a supercontinuum pumped into anomalous dispersion. Results of the interferometric measurements of the coherence degree, discussed earlier, are in disagreement with this scenario, though. The applicant sought an additional support for his claim, and referred to numerical simulations of nonlinear propagation. GNLSE simulations are usually applied to cases limited to the fundamental mode propagation, because GNLSE is scalar. This is why the coherent seeding of supercontinuum generation from the photonic cladding of an all-solid photonic crystal fiber was represented numerically using a vector variant of the GNLSE (MM-GNLSE – multi-mode GNLSE). Each mode considered in the model is then represented with one GNLSE and a set of linear parameters – the group velocity and its dispersion, as well as its own nonlinear coefficient γ. The value of γ depends on the effective mode area of the given mode. This reflects the property, where the fundamental mode (small effective mode area) experiences strong nonlinearity, while the given higher order mode in the photonic cladding is propagated linearly (due to large effective area and consequently small value of γ). Moreover, the MM-GNLSE equations are coupled with modal coupling coefficients. The values of dispersion parameters and mode coupling coefficients can be obtained from numerical simulations of the known fiber structure and material parameters of the fiber glasses (material dispersion). The mathematical form of the MM-GNLSE model (4) was proposed by the authors of papers [46-48]:

$$\frac{\partial A_p(z,T)}{\partial z} = [i\left(\beta_0^{(p)} - \beta_0\right)A_p(z,T) - \left(\beta_1^{(p)} - \beta_1\right)\frac{\partial A_p(z,T)}{\partial T} + i\sum_{n\geq 2}\frac{1}{n!}\beta_n^{(p)}\frac{i^n\partial^n A_p(z,T)}{\partial T^n}]$$

$$+[i\frac{n_2\omega_0}{c}\sum_{l,m,n}\left\{\left(1 + i\tau_{plmn}^{(1)}\frac{\partial}{\partial T}\right)Q_{plmn}^{(1)}2A_l(z,T)\int R(T')A_m(z,T-T')A_n^*(z,T-T')dT'\right.$$

$$\left.+\left(1 + i\tau_{plmn}^{(2)}\frac{\partial}{\partial T}\right)Q_{plmn}^{(2)}2A_l^*(z,T)\int R(T')A_m(z,T-T')A_n(z,T-T')e^{2i\omega_0 T'}dT'\right\}]$$

$$\tag{5}$$

$$Q_{plmn}^{(1)}(\omega) = \frac{\varepsilon_0^2 n_0^2 c^2}{12}\frac{\iint\left[E_p^*(\omega)\cdot E_l(\omega)\right]\left[E_m(\omega)\cdot E_n^*(\omega)\right]dS}{N_p(\omega)N_l(\omega)N_m(\omega)N_n(\omega)}$$

$$Q_{plmn}^{(2)}(\omega) = \frac{\varepsilon_0^2 n_0^2 c^2}{12}\frac{\iint\left[E_p^*(\omega)\cdot E_l^*(\omega)\right]\left[E_m(\omega)\cdot E_n(\omega)\right]dS}{N_p(\omega)N_l(\omega)N_m(\omega)N_n(\omega)}$$

where β_0, β_1, β_n – are the dispersion parameters of the modes (superscript „(p)" denotes higher order mode), Q_{plmn} are the complex mode coupling coefficients. The remaining symbols are consistent with the scalar GNLSE, where A stands for the complex field amplitude, z – the propagation coordinate, T – time, n_2 – nonlinear refractive index, c – speed of light in vacuum, ω_0 center angular frequency of the simulation window (usually also the center frequency of the pump pulse) R – the delayed Raman response, and τ_{plmn} – the self-steeping time scale, dependent on the effective mode area.

The numerical load of the MM-GNLSE model is very large and can be prohibitive even on modern, up-to-date computers. For this reason the applicant decided to implement a model with only the fundamental mode and one single higher order mode from the cladding considered in the simulations. The calculations were performed for supercontinuum generation in the two cases: a) using a scalar GNLSE model with only the fundamental mode's chromatic dispersion of the fiber core of the NL21 ANDi fiber, b) for the same fiber the applicant prepared calculations using the MM-GNLSE (vector) model taking into account the fundamental mode and one higher order mode from the photonic lattice. The pump pulse energy considered in the core of the fiber was the same in both types of simulations. It was assumed also, that during the in-coupling of pump light into the NL21 fiber, 25% of the pulse energy couples and continues propagation in the photonic cladding, and the remainder of 75% couples and propagates in the core. In order to meet the assumption of equal energies in the fiber core in both simulations, the total pump pulse energy in-coupled to the fiber in the vector simulation was therefore accordingly increased. The results of the simulations are presented in Fig. 13. Four simulations were conducted with each of the model, for in-coupled pulse energies in the core of 2, 3, 4 and 5 nJ (that is respectively 2.85, 4.29, 5.72, 7.15 nJ total in-coupled energy into the fiber in the vector simulations). As expected, the spectrum in the scalar simulation maintains high coherence only for the lower pulse energies, specifically when the spectrum is limited to the self-seeded SPM effect. As soon as the side bands begin to appear, noise is amplified across the spectrum, with the long-wavelength part being especially affected, which is typical for Raman scattering and has been observed before by other groups [49]. As can be seen in the individual spectral characteristics in Fig. 13a, the phase fluctuations are accompanied by intensity fluctuations. The spectrum generated in the vector simulations remains coherent in terms of phase and intensity across all investigated pump pulse energies. Specifically, noise amplification is avoided, as in the experiment, even when the spectrum width exceeds the limit of SPM domination. This supports the applicant's claim on the stabilizing role played by the cladding mode (photonic lattice mode) in a nonlinear, double-clad photonic crystal fiber for supercontinuum generated in the fundamental mode of the core. **To the best of the applicant's knowledge, he was the first to describe higher-order mode contribution to improving the coherence of the fundamental mode.**

Spectral correlation maps calculated for the pump pulse energy of 4 nJ (scalar simulation) and 5.72 nJ (vector simulation) are presented in Fig. 14. The clearly seen areas of correlated wavelengths on the scalar simulation map (Fig. 14a) are related to the incoherent growth of the FWM-Raman side bands at the Stokes and anti-Stokes sides of the pump wavelength [MK-6]. Correlation pattern of the vector simulation is different. The correlation of the spectrum from the vector simulation (Fig. 14b) contains a regular structure of correlated spots, located at both the short-wavelength and long-wavelength sides of the spectrum (detail close-ups shown in Fig. 14b). The pattern in Fig. 14b is different than in the maps from the experimental DFT data (Fig. 11b,c), but their common feature is the presence of a rectangular grid structure of correlated areas. The vector simulation included only one mode from the photonic cladding, which could be delivering the deterministic seed signal. The real fiber structure supports simultaneously multiple higher order modes with an overlap to the core. Correlation pattern obtained from experimental data (Fig. 11.b,c) is therefore a result of a spatio-temporal average of influence of many modes with different dispersion characteristics, different group velocity mismatch with the core mode, and which interact with the core mode at different fragments of propagation along the fiber, with different mode couplings.
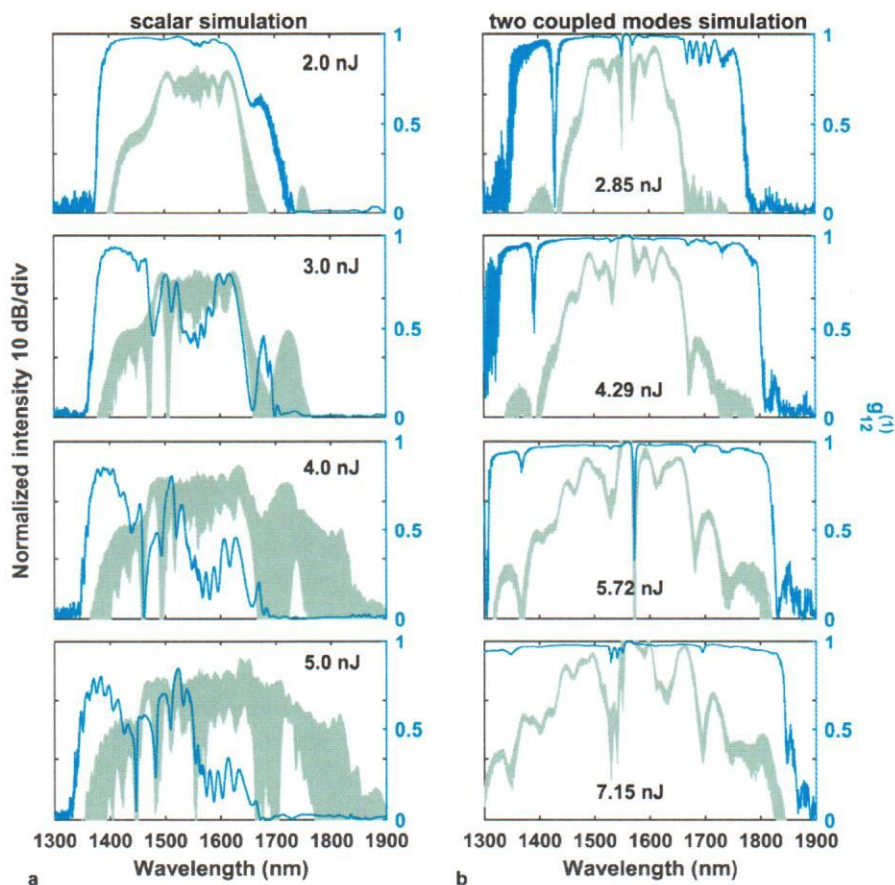

Fig. 13. Supercontinuum spectra obtained from numerical simulations using modelling a) with scalar GNLSE and b) with vector GNLSE. Each plot shows an ensemble of 500-shot realization with stochastic initial condition in the pump pulse (one photon per mode noise) and the corresponding modulus of the complex degree of coherence. The energies given in the plots are energies in-coupled to the fiber. [MK-7]
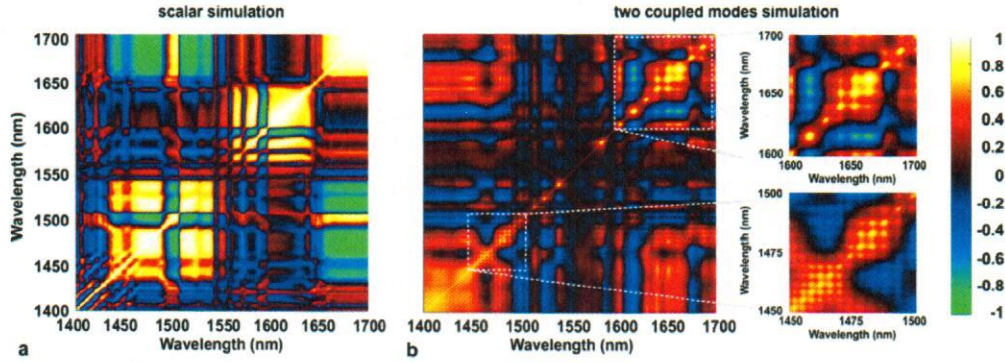
Fig. 14. Spectral correlation maps calculated for the ANDi supercontinuum using numerically obtained ensembles of spectra, modelling with a) scalar GNLSE, b) vector, MM-GNLSE.

The results obtained by the applicant are important for the community of engineers working on new broadband sources, and for scientists relying on such sources in their work in the areas of life sciences or strict sciences. They indicate the feasibility of constructing ultra-stable supercontinuum sources, in which the energy source would not be a costly and complex femtosecond laser without any portability, but a compact and robust picosecond laser with high average output power.

Initial pulse parameters and the properties of all-normal dispersion supercontinuum

In parallel to the above, the applicant and team conducted research on how the initial pulse parameters influence the spectral characteristics of supercontinuum generation in all-normal dispersion fibers. This part of research was mainly theoretical in nature and was supposed to provide feedback to the development work of the nonlinear fibers of the following series.

In the work [**MK-8**] the applicant with the team from ITME and with collaborators from Tyndall National Institute in Cork, Ireland, investigated the impact of steepness of the pump pulse's temporal envelope edge, on the shape of the spectral characteristic and correlation picture of an ANDi supercontinuum. The research involved scalar GNLSE simulations with the initial pulse given in the form of equations (6) and (7):

$$\begin{cases} P(T) = P_{peak} \cdot \exp\left[-4 \cdot (\ln 2) \cdot \left(\frac{T}{0.05 \cdot T_0}\right)^2\right] & T < 0 \\ P(T) = P_{peak} \cdot \exp\left[-4 \cdot (\ln 2) \cdot \left(\frac{T}{1.95 \cdot T_0}\right)^2\right] & T \geq 0 \end{cases} \tag{6}$$

$$\begin{cases} P(T) = P_{peak} \cdot sech^2\left(\frac{T}{0.05 \cdot T_0}\right) & T < 0 \\ P(T) = P_{peak} \cdot sech^2\left(\frac{T}{1.95 \cdot T_0}\right) & T \geq 0 \end{cases} \tag{7}$$

Both pulses were built based on regular Gaussian (6) and $sech^2$ (7) shapes. Steepness of the leading edge was intentionally introduced in both envelopes (leading temporal edge for the wavelengths with normal dispersion). Pulse deformations of this type can exist in real laser systems and the applicant's goal with the work [**MK-8**] was to explore their consequences to supercontinuum properties, such as coherence, flatness of spectrum or spectral correlation. Time duration of the not deformed pulses was 180 fs (Raman scattering therefore did not play the dominant role in the spectral broadening).

In the work, spectral correlation analysis was used to explain how the temporal pulse shape of the pump influenced the interaction of OWB and SPM during formation of an ANDi spectrum. The correlation patterns shown in Fig. 14a, calculated for the analytical Gaussian profiles of the initial pulse, contained clear oval features, size of which depended on the steepness of the pump pulse edge. The less steep pulse edge (the leading edge) of a Gaussian profile resulted in the short-wavelength side-band of the ANDi spectrum generated at a much lower intensity, than the central part of spectrum shaped

by the SPM. This was due to a broader band of OWB and the generation of the side band with SPM components with more detuning from the pump wavelength. When the initial pulse had the sech^2 profile, the applicant explained how the less slope in the wings of this pulse profile, compared to a Gaussian profile, led to the energy of the SPM pulse being transferred to a narrower range of wavelengths. For the less steep, trailing edge of the considered sech^2 pulse shape, the generated short-wavelength part of the spectrum was separated from the central part of SPM-broadened spectrum by a pronounced intensity-dip. Rectangular shape of OWB features in the correlation map for this case (Fig. 15.b) corresponded to a situation, when the wings of the sech^2 pulse with more intensity (that a Gaussian pulse shape) were generating a gradient in the range of wavelengths taking part in the parametric interaction of the supercontinuum side-bands.
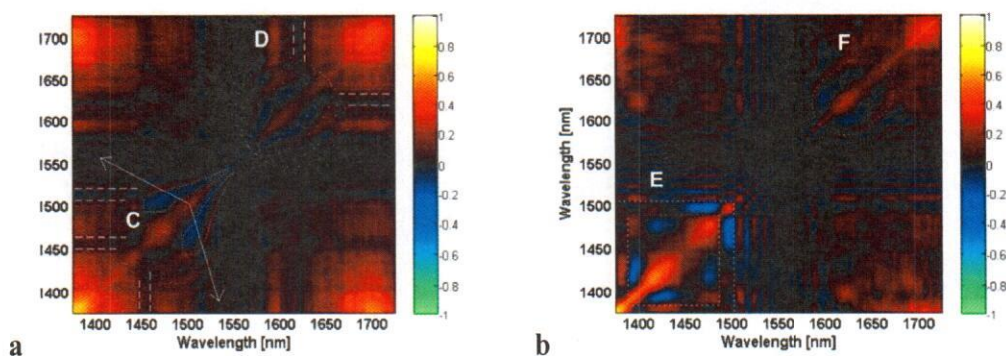

Fig. 15. Spectral correlation maps for numerical ANDi supercontinuum spectrum, assumed pumping by around 180 fs long pules with intentionally introduced steepness at one of the edges, a: Gaussian-based initial pulse (6), b: sech^2 based initial pulse (7).

The analysis of the degree of coherence of the separated side band of supercontinuum spectrum revealed also a property, that the asymmetric pump pulse (steepened at one of the edges) led to a transferring of the pump laser shot noise to the part of ANDi spectrum, which in the time domain was related to the steepened pulse edge.

In scope of work [MK-8], the applicant conducted a versatile analysis of the influence of the pump pulse temporal envelope on the spectral and coherence properties of the ANDi supercontinuum spectrum in fibers with flattened normal dispersion profile. An important and universal conclusion of the work for the area of research on generation and application of supercontinuum is the observation, that while theoretically the shape of the supercontinuum spectrum stabilizes at a similar (or even the same) level, regardless of the temporal profile of the pump pulse (Gaussian or sech^2), the propagation distance along the nonlinear fiber when a sech^2 pulse is used, would be much longer than for the Gaussian initial pulse. With silica photonic crystal fibers, where the loss would be at the level of single (or a fraction of) dB/km at most and supercontinuum generation is achieved over meters of length of the fiber, it is of secondary importance. Silica glass however, does not allow for supercontinuum generation in the attractive mid-infrared spectral range. Transmission in the mid-infrared is possible in fluoride glass fibers. Their propagation losses can be even lower than in silica telecommunication fibers, but the dispersion engineering in fluoride glass fibers is challenging due to recrystallization of the glass. Other soft glasses made of various oxides of heavy metals, or non-oxide glasses of sulfides, selenides or tellurides, have a broad transmission window up to several (or even over 20) micrometers, but the fibers drawn from these glasses typically have attenuation at a level of dB/m. In media like these, it is desirable to shorten the propagation length and the faster development of an ANDi supercontinuum spectrum using a Gaussian pump pulse shape in such fibers is of critical importance.

The work [MK-8] was featured by the publisher – IOP Publishing as IOP SELECT, shortly after publication. This collection includes the best and the most important research papers published by IOP Publishing in the preceding 12 months. Next, the editors of Journal of Optics decided to include the work

in a special issue of the journal, the Journal of Optics Highlights 2014. The Highlights series contains the best research papers published in the given IOP journal during a particular year.

In the work [**MK-9**] Bartłomiej Siwicki, MSc, under the supervision of the applicant, investigated the linear properties of all-solid glass ANDi photonic crystal fibers for different pairs of thermally matched glasses. Two pairs of glasses were studied: the boron-silicate glass (designated NC21A), which was the lattice filling of the NL21 series of fibers, and two commercial glasses, F2 and SF6 from Schott. The so-far studied pair of NC21A (lattice inclusions) and F2 (core and lattice pattern) served as the reference point to explore two new combinations: NC21A (inclusions) and SF6 (core and lattice pattern), as well as F2 (inclusions) and SF6 (again core and lattice pattern). Selected results of numerical simulations of linear properties (chromatic dispersion profiles depending on geometrical parameters of lattice) are shown in Fig. 16.
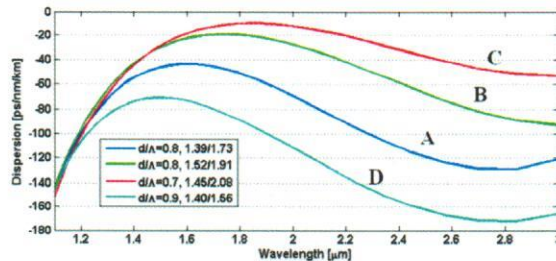

Fig. 16. Selected results of linear simulations of dispersion properties of ANDi fibers made from F2 and SF6 glasses (glasses offered by Schott).

The result of this research was the selection of the most attractive structure in the context of the nonlinearity of the core, the refractive index contrast between the pair of glasses used for the designing and the shape of the dispersion profile. The structure was fabricated by the applicant's team at ITME and is presently under investigation by B. Siwicki and the applicant in context of the influence of chromatic dispersion profile and the frequency dependence of the effective mode area on the spectral and coherence properties of ANDi supercontinuum. The approach to fabrication of fibers for efficient generation of coherent supercontinuum, based on the designing of all-solid glass photonic crystal fibers is practiced by just a handful of research groups in the world, including the team of the applicant. The problem of engineering of the effective mode area dependence on wavelength is a completely new issue and is one of the current threads of research of the applicant and collaborators (discussed in detail later). Further research results in this field are to appear in a full text paper and in parallel will be contained in the PhD dissertation prepared by B. Siwicki.

In the work [**MK-10**] B. Siwicki with the applicant investigated the influence of the initial pulse parameters, such as the pump pulse energy and peak power, on the flatness and width of the ANDi supercontinuum spectrum in NL21 series ANDi fibers. The paper is a record on an analysis of the results of numerical simulations conducted using the scalar GNLSE model. The criterion for selection of the initial pulse parameters was the commercial availability or laboratory accessibility in form of a working laser setup designed and built by the applicant's collaborators from the Laser and Fiber Electronics Group of prof. K. M. Abramski from Wroclaw University of Technology. The results obtained in course of this work were used during the designing and building of laser setups for use as pump sources in other research work on supercontinuum generation by the applicant's group in collaboration with prof. Abramski's group.

Nanostructuring of fiber core as new means of dispersion and effective mode area engineering

The most recent results of research done by the applicant and collaborators suggest significance of the engineering of the effective area dependence on wavelength, on par with dispersion engineering. The changes of both characteristics due to manipulation with the transverse geometry of the structure, are nevertheless strongly related. It can be a limitation in the designing of a nonlinear fiber for ANDi

supercontinuum generation. Moreover, there is a limited number of glass compositions with a satisfactory refractive index contrast, which enable joint thermal processing into structured fibers.

The applicant's research group reported for the first time of a nanostructured core optical fiber in the recent paper [MK-11]. The core of the fiber was composed of about 8000 glass rods from two types of boron-silicate glasses with refractive indices of $n_D = 1.5273$ and $n_D = 1.5581$. The approach used by the applicant's group is based on the effective medium theorem. According to it, the refractive index distribution experienced by the wave propagated in the structure, stems from an effective value of refractive index shaped by the distribution of the structure's constituent elements, as long as these elements are sub-wavelength in size. The team designed the distribution profile of the elements in the structure according to the assumed parabolic profile of refractive index. The structure topology and theoretical refractive index profile are shown in Fig. 17a,b. The stacked fiber core preform is shown in Fig. 17c. It was 6 cm long at the longer diagonal, and a single rod was 0.6 mm in diameter. The long diagonal contains exactly 100 rods. After drawing at a fiber drawing tower, the preform had a diameter of about 2.5 mm (depending on a particular sample and intended follow-up processing) – Fig. 17d. Before drawing into the final fiber, this sub-preform was placed in a lower-refractive index glass tube. The series of drawn optical fibers comprised several samples with different diameter of the nanostructured core, ranging from about 3 µm to 7 µm. The outer diameters were in the range from 74 µm to 120 µm and depended on the process conditions. Their variation from sample to sample (not along a single sample!) did not influence the dispersive properties of the fibers. The geometrical parameters of the fabricated fibers are presented in Tab. 2, and the SEM images of selected final fibers are shown in Fig. 18.
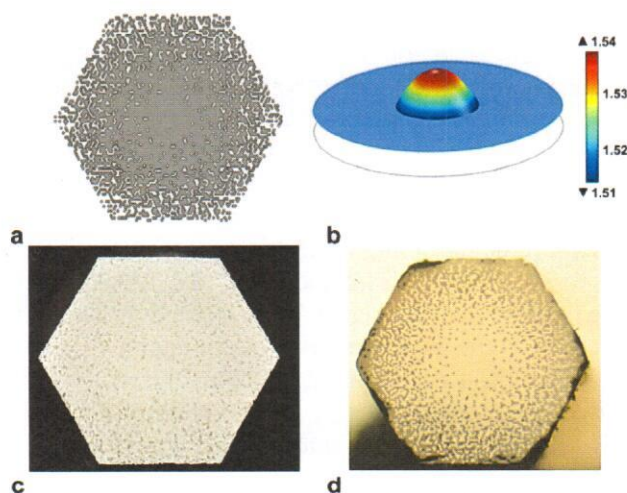

Fig. 17. a: Design of the core nanostructure, b: theoretical distribution of the refractive index in the core, c: stacked preform of fiber core, d: core preform drawn at a fiber drawing tower.
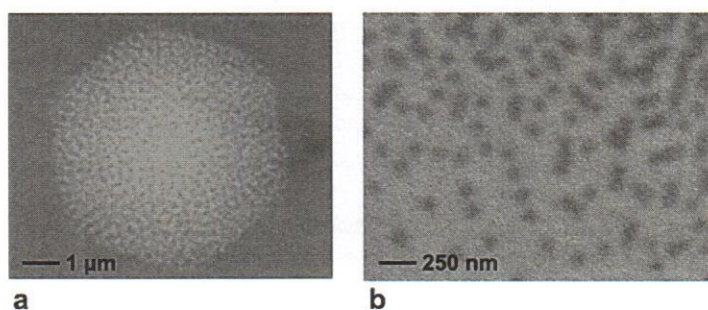

Fig. 18. SEM images of the final nanostructured core fibers, a: core area, b: detail of nanostructure.

Table 2. Geometrical parameters of the fabricated nanostructured core fibers [MK-11].

No	Outer diameter	Core dimensions
1	74.2 μm	6.9 × 6.0 μm
2	58.5 μm	5.4 × 4.9 μm
3	122.2 μm	4.0 × 4.4 μm
4	110.3 μm	3.7 × 4.2 μm
5	100.9 μm	3.3 × 3.9 μm
6	90.16 μm	2.8 × 3.2 μm

Initially, the applicant's team assumed performing a technological trial of fabricating an optical fiber with arbitrarily arranged transverse refractive index profile. The refractive index profile in the fabricated fibers was symmetric against the axis of the fiber, but it is possible to create other, asymmetric topologies of gradient index fibers using the same technological platform. The applicant's group noted, that in the fabricated test series of fibers the dispersion profile followed a reversed trend of evolution with changes of the core dimension, to what is known from the existing literature. The zero dispersion point was red-shifting and then disappearing altogether (the dispersion profile moving into all-normal range of values – within the studied wavelength range) along with decreasing of the core diameter, as shown in Fig. 19.
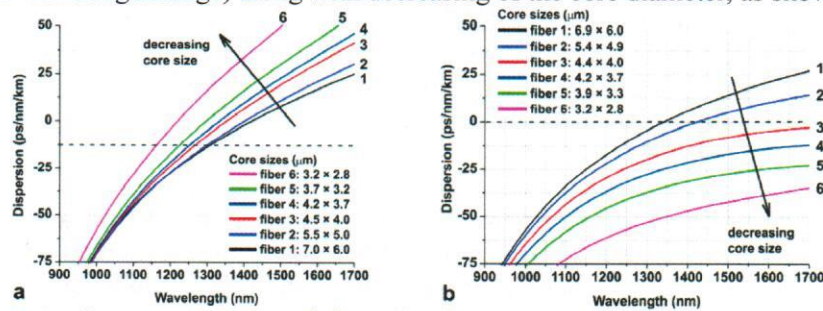

Fig. 19. a: Chromatic dispersion estimated from the design of the nanostructured core fibers based on numerical simulations – result consistent with the state-of-the-art; b: the dispersion profiles measured in the fabricated fibers.

Results of energy-dispersive X-ray spectroscopy (EDS) measurements on the fiber samples revealed a process of selective diffusion of certain atoms of the chemical composition of the core glasses. As a result, the spatial profiles of distribution of atoms including barium, silicon and oxygen in the boron-silicate glasses are changed at the nanostructure level, compared to the drawn preform of the core. Further consequence is that in the final fiber, there is a change of the material dispersion contribution of the nanostructure in the core. This hypothesis is confirmed by numerical simulations, in which the material dispersion profile was modified within the nanostructured core area. It turned out, that the use of one of such optimized material dispersion profiles allowed to numerically reconstruct both the initially assumed parabolic distribution of the refractive index profile (shaped primarily by the barium atom concentration) and the trend of evolution of the fiber dispersion with the change of the nanostructured core dimension. These results are shown in Fig. 20.
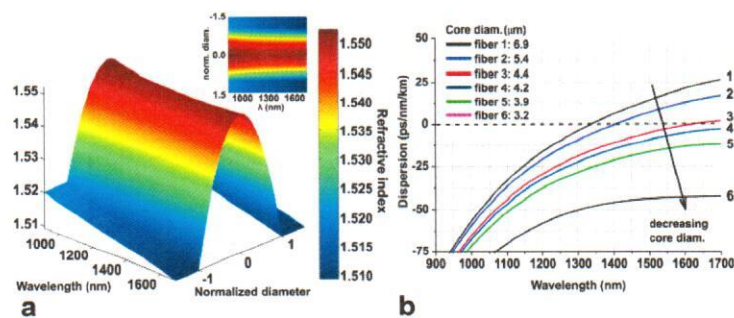
Fig. 20. a: Spatial and spectral profile of the effective refractive index in the nanostructured core of fiber (geometric dependence shown as dependence on the normalized diameter), b: chromatic dispersion profiles calculated for the fibers with different core diameters for an optimized material dispersion at the core nanostructure level.

Results reported in the paper [**MK-11**] are of universal significance. It has been shown that there existed another means of shaping of the effective mode area in an optical fiber (related to the core diameter) against the changes of the chromatic dispersion profile. Moreover, an experimental demonstration of refractive index profile shaping in an arbitrary manner has been reported. It was not constrained to any axial symmetry nor to any other limitations known from the gradient index fiber technology. The applicant's contribution in the work [**MK-11**] was fabrication of the nanostructured core fibers, measurements of supercontinuum generation which in the text of paper were used to verify the trend of evolution of the dispersion profile, and the analysis and discussion of all theoretical and experimental results, as well as writing and corrections of the manuscript.

Summary

The cycle of research papers related in scope and subject, entitled "Impact of the dispersion characteristics of the nonlinear medium and of the initial pump pulse condition on the spectral and coherence properties of the supercontinuum", presented by the applicant, includes new research results on generation of stable supercontinuum. The scope of work encompasses characterization of coherence and spectral properties, as well as the development of glass synthesis and photonic crystal fibers technologies, allowing for the use of high energy picosecond pulse pumping from fiber lasers. The applicant also proposed a new means to preserving the phase coherence in pumping conditions favoring noise amplification, as well as a new approach to the designing of structured fibers with predefined propagation properties. During his work with the ITME research group, the applicant participated in all stages of the research: starting with theoretical work with the use of linear and nonlinear modelling, through experiment, up to technological work on the development of nonlinear and nanostructured core photonic crystal fibers.

Literature (excluding papers of the applicant's cycles of research publications)

[1] Dudley J. M. & Coen S. Coherence properties of supercontinuum spectra generated in photonic crystal and tapered optical fibers. Opt. Lett. 27, 1180-1182 (2002).

[2] Møller U. & Bang O. Intensity noise in normal-pumped picoseconds supercontinuum generation, where higher-order Raman lines cross into the anomalous dispersion regime. Electron. Lett. 49, 63-65 (2013).

[3] L. G. Wright, D. N. Christodoulides, and F. W. Wise, "Controllable spatiotemporal nonlinear effects in multimode fibres," Nature Photon. 9, 306–310, (2015).

[4] S. Ishida, N. Nishizawa, Quantitative comparison of contrast and imaging depth of ultrahigh-resolution optical coherence tomography images in 800–1700 nm wavelength region, Biomedical Optics Express 3, 282-294 (2012)

[5] Y. Takushima, K. Kikuchi, 10-GHz Over 20-Channel Multiwavelength Pulse Source by Slicing Super-Continuum Spectrum Generated in Normal-Dispersion Fiber, IEEE Photonics Technology Letters 11, 322-324 (1999).

[6] Sun Y. et al. Characterization of an orange acceptor fluorescent protein for sensitized spectral fluorescence resonance energy transfer microscopy using a white-light laser. J. Biomed. Opt. 14, 054009 (2009).

[7] Utkarsh Sharma, Ernest W. Chang, and Seok H. Yun, Long-wavelength optical coherence tomography at 1.7 μm for enhanced imaging depth, Opt. Express 16, 19712-19723 (2008).

[8] H. Kawagoe, S. Ishida, M. Aramaki, Y. Sakakibara, E. Omoda, H. Kataura, and N. Nishizawa, Development of a high power supercontinuum source in the 1.7 μm wavelength region for highly penetrative ultrahigh-resolution optical coherence tomography, Biomedical Optics Express 5, 932-943 (2014).

[9] Cheung C. S., Daniel J. M. O., Tokurakawa M., Clarkson W. A. & Liang H. High resolution Fourier domain optical coherence tomography in the 2 μm wavelength range using a broadband supercontinuum source. Opt. Express 23, 1992-2001 (2015).

[10] Rui Wu, Victor Torres-Company, Daniel E. Leaird, Andrew M. Weiner, Supercontinuum-based 10-GHz flat-topped optical frequency comb generation, Opt. Express 21, 6045-6052 (2013).

[11] Chen-Bin Huang, Sang-Gyu Park, Daniel E. Leaird, and Andrew M. Weiner, Nonlinearly broadened phase-modulated continuous-wave laser frequency combs characterized using DPSK decoding, Opt. Express 16, 2520-2527 (2008).

[12] R. R. Alfano, S. L. Shapiro, "Emission in the Region 4000 to 7000 Å Via Four-Photon Coupling in Glass," Phys. Rev. Lett. 24(11), 584-587 (1970).

[13] Dudley J. M., Genty G. & Coen S. Supercontinuum generation in photonic crystal fiber. Rev. Mod. Phys. 78, 1135-1184, (2006).

[14] G. P. Agrawal, Nonlinear Fiber Optics, Third Edition, Academic Press 2001.

[15] M. Trippenbach and Y. B. Band, Effects of self-steepening and self-frequency shifting on short-pulse splitting in dispersive nonlinear media, Phys. Rev. A 57, 4791 (1998)

[16] D. Anderson, M. Desaix, M. Lisak, and M. L. Quiroga-Teixeiro, Wave-breaking in nonlinear optical fibers, J. Opt. Soc. Am. B 9, 1358–1361 (1992)

[17] N. Akhmediev, M. Karlsson, Cherenkov radiation emitted by solitons in optical fibers, Phys. Rev. A 51, 2602 (1995).

[18] J. M. Dudley and J. R. Taylor, editors, Supercontinuum Generation in Optical Fibers, (Cambridge 2010).

[19] R. H. Stolen, J. P. Gordon, W. J. Tomlinson, H. A. Haus, Raman response function of silica-core fibers, J. Opt. Soc. Am. B 6, 1159-1166 (1989)

[20] P. Domachuk, N. A. Wolchover, M. Cronin-Golomb, A. Wang, A. K. George, C. M. B. Cordeiro, J. C. Knight, F. G. Omenetto, Over 4000 nm bandwidth of Mid-IR supercontinuum generation in sub-centimeter segments of highly nonlinear tellurite PCFs, Optics Express 16 (2008), 7161-7168.

[21] C. Agger, C. Petersen, S. Dupont, H. Steffensen, J. K. Lyngsø, C. L. Thomsen, J. Thøgersen, S. R. Keiding, O. Bang, "Supercontinuum generation in ZBLAN fibers—detailed comparison between measurement and simulation," J. Opt. Soc. Am. B 29(4), 635-645 (2012).

[22] Petersen C. R. et al. Mid-infrared supercontinuum covering the 1.4–13.3 μm molecular fingerprint region using ultra-high NA chalcogenide step-index fibre. Nature Photon. 8, 830-834 (2014).

[23] T. Godin, Y. Combes, R. Ahmad, M. Rochette, T. Sylvestre, and J. M. Dudley, "Far-detuned mid-infrared frequency conversion via normal dispersion modulation instability in chalcogenide microwires," Opt. Lett. 39(7), 1885-1888 (2014).

[24] Domingue S. R. & Bartels R. A. Overcoming temporal polarization instabilities from the latent birefringence in all-normal dispersion, wave-breaking-extended nonlinear fiber supercontinuum generation. Opt. Express 21, 13305-13321 (2013).

[25] Liu Y. et al. Suppressing short-term polarization noise and related spectral decoherence in all-normal dispersion fiber supercontinuum generation. J. Lightwave Technology DOI: 10.1109/JLT.2015.2397276 (2015).

[26] Sørensen S. T. et al. The role of phase coherence in seeded supercontinuum generation. Opt. Express 20, 22886-22894 (2012).

[27] Nguyen D. M. et al. Incoherent resonant seeding of modulation instability in optical fiber. Opt. Lett. 38, 5338-5341 (2013).

[28] Ren Z., Xu Y., Qiu Y., Wong K. K. Y. & Tsia K. Spectrally-resolved statistical characterization of seeded supercontinuum suppression using optical time-stretch. Opt. Express 22, 11849-11860 (2014).

[29] Falk P., Frosz M. H. & Bang O. Supercontinuum generation in a photonic crystal fiber with two zero-dispersion wavelengths tapered to normal dispersion at all wavelengths. Opt. Express 13, 7535-7540 (2005).

[30] Li F., Li Q., Yuan J. & Wai P. K. A. Highly coherent supercontinuum generation with picosecond pulses by using self-similar compression. Opt. Express 22, 27339-27354 (2014).

[31] Hooper L. E., Mosley P. J., Muir A. C., Wadsworth W. J. & Knight J. C. Coherent supercontinuum generation in photonic crystal fiber with all-normal group velocity dispersion. Opt. Express 19, 4902-4907 (2011).

[32] Heidt A. M. et al. Coherent octave spanning near-infrared and visible supercontinuum generation in all-normal dispersion photonic crystal fibers. Opt. Express 19 3775-3787 (2011).

[33] Nishizawa N. & Takayanagi J. Octave spanning high-quality supercontinuum generation in all-fiber system. J. Opt. Soc. Am. B 24, 1786-1792 (2007).

[34] K. Chow, Y. Takushima, C. Lin, C. Shu, and A. Bjarklev, Flat supercontinuum generation based on normal dispersion nonlinear photonic crystal fiber, Electron. Lett. 42, 989 (2006).

[35] Xia Li, Wei Chen, Tianfeng Xue, Juanjuan Gao, Weiqing Gao, Lili Hu, Meisong Liao, Low threshold mid-infrared supercontinuum generation in short fluoride-chalcogenide multimaterial fibers Opt. Express 22, 24179-24191 (2014).

[36] A. M. Heidt, "Pulse preserving flat-top supercontinuum generation in all-normal dispersion photonic crystal fibers", J. Opt. Soc. Am. B 27(3), pp. 550-559 (2010).

[37] X. Feng, T.M. Monro, P. Petropoulos, V. Finazzi, D. Hewak, "Solid microstructured optical fiber", Opt. Express 11(18), pp. 2225-2230 (2003).

[38] R. Buczyński, J. Pniewski, D. Pysz, R. Stępień, R. Kasztelanic, I. Kujawa, A. Filipkowski, A. J. Waddie, M. R. Taghizadeh, Dispersion management in soft glass all-solid photonic crystal fibres, Optoelectronic Review 20(3), 207–215 (2012).

[39] Lorentz D. et al. Nonlinear refractive index of multicomponent glasses designed for fabrication of photonic crystal fibers. Appl. Phys. B 93, 531–538 (2008).

[40] T. Martynkien, D. Pysz, R. Stępień, and R. Buczyński, "All-solid microstructured fiber with flat normal chromatic dispersion," Opt. Lett. 39(8), pp. 2342–2345 (2014).

[41] R. Stępień, J. Cimek, D. Pysz, I. Kujawa, M. Klimczak, and R. Buczyński, Soft glasses for photonic crystal fibers and microstructured optical components, Opt. Eng. 53 (7), 071815 (2014).

[42] G. Sobon, Mode-locking of fiber lasers using novel two-dimensional nanomaterials: graphene and topological insulators [Invited], Photonics Research 3, A56-A63 (2015)

[43] Goda K. & Jalali B. Dispersive Fourier transformation for fast continuous single-shot measurements. Nature Photon. 7, 102-112 (2013).

[44] Wetzel B. et al. Real-time full bandwidth measurement of spectral noise in supercontinuum generation. Sci. Rep. 2:882 10.1038/srep00882 (2012).

[45] Godin T. et al. Real time noise and wavelength correlations in octave-spanning supercontinuum generation. Opt. Express 21, 18452-18460 (2013).

[46] Poletti F. & Horak P. Description of ultrashort pulse propagation in multimode optical fibers. J. Opt. Soc. Am. B 25, 1645-1654 (2008).

[47] Poletti F. & Horak P. Dynamics of femtosecond supercontinuum generation in multimode fibers. Opt. Express 17, 6134-6147 (2009).

[48] Khakimov R., Shavrin I., Novotny S., Kaivola M., Ludvigsen H. Numerical solver for supercontinuum generation in multimode optical fibers. Opt. Express 21, 14388- 14398 (2013).
[49] Aalto A., Genty G. & Toivonen J. Extreme-value statistics in supercontinuum generation by cascaded stimulated Raman scattering. Opt. Express 18, 1234-1239 (2010).

5. Discussion of other scientific achievements
a) achievements before obtaining of the PhD degree

For his PhD thesis, the applicant investigated upconversion pumping schemes, leading to the visible emission under infrared excitation, including laser diode pumping, in various glassy and crystalline, rare-earth doped systems. Advisor for this work was prof. Michał Malinowski. Specifically, the applicant studied trivalent neodymium and trivalent holmium doped ZBLAN glasses for UV-violet emission. For the first time to the best of the applicant's knowledge, together with advisor and collaborators, he reported the fluorescence lifetimes of energy levels, from which the 4f-4f UV-violet optical transitions take place in Nd^{3+} ions doped in ZBLAN glass [Pir2006, Kli2012]. He also investigated trivalent-dysprosium doped YAG/YAG planar waveguides [Kli2009] – a paper later cited by international groups in context of yellow-emitting lasers, optically active powders for lighting systems or temperature sensors. The research conducted by the applicant during his PhD program included also investigation of short-wavelength emission properties of ZBLAN glasses and fibers doped with other trivalent lanthanides, such as erbium, thulium and dysprosium, and co-doped with praseodymium and ytterbium. The applicant took part in measurements of excited state absorption in ZBLAN glasses doped with neodymium or holmium ions. Results were reported in peer-reviewed journals included in the JCR list – these are the papers listed in a following section of this statement, p. c) "Research papers published before obtaining of the PhD degree".

Together with his PhD thesis advisor and collaborators, he was awarded Rector Team Awards for scientific excellence at Warsaw University of Technology (twice: in 2008 and 2010). He also received a special scholarship for the excelling PhD students, awarded at a Voivodeship level in Poland, for his research achievements.

Literature (selected papers)
[Pir2006] R. Piramidowicz, P. Witoński, M. Klimczak, M. Malinowski, „Analysis of up-converted UV fluorescence dynamics in Nd^{3+} doped ZBLAN glasses," Optical Materials 28(1), 152-156 (2006).
[Kli2009] M. Klimczak, M. Malinowski, J. Sarnecki, R. Piramidowicz, „Luminescence properties in the visible of Dy: YAG/YAG planar waveguides," Journal of Luminescence 129(12), 1869-1873 (2009).
[Kli2012] M. Klimczak and R. Piramidowicz, „UV-violet emission properties of $^2F(2)_{5/2}$ energy level of Nd^{3+} ions in ZBLAN glass," Applied Physics B 106(4), 1019-1025 (2012).

b) achievements after obtaining of the PhD degree

After completing his PhD program and obtaining the PhD degree, the applicant transferred into the area of research on semiconductor laser materials and devices. The group was, and presently is, headed by prof. Witold A. Trzeciakowski. Specifically, the applicant took part in research and development work on widely tunable laser diodes, where the wavelength tuning function was achieved using application of high hydrostatic pressure. This experimentally difficult technique of manipulation with properties of operational semiconductor laser devices is available to only a few research groups in the world. During his time with the group, the applicant and collaborators demonstrated continuous tenability of high power laser diode chips (1-3 W of continuous wave output power) covering the entire range of 720-1540 nm [Dyb2013], they studied and described current leakage mechanics in these conditions [Ber2013] and demonstrated an application of the developed laser devices in spectroscopy of laser materials [Ber2013a]. Finally, they performed extensive research of reliability and failure mechanisms of laser diode chips operating in these difficult conditions [Ber2014] – this paper appeared online after the applicant's departure from this research group (although he took part in all research work and in preparation, as well as corrections of the manuscript).

Being a part of this group was a unique opportunity for the applicant to gain extensive experimental experience with near-infrared optical and spectroscopic measurements, and to work with unique but technically very unforgiving equipment. It was also an opportunity to gain experience in preparation and running of a larger research and development project: together with the group Head, the applicant co-authored the grant proposal "Adaptation of laser diodes tunable with high hydrostatic pressure to market demands", which was funded by National Center for Research and Development in Poland (about 450.000,00 EUR, 2011-2014).

The applicant transferred to the present research group of prof. R. Buczyński at ITME, at the end of 2012.

Literature

[Dyb2013] F. Dybala, A. Bercha, M. Klimczak, B. Piechal, Y. Ivonyak, W. A. Trzeciakowski, "Pressure tuning of high-power laser diodes in the 720–1540 nm range," physica status solidi (b) 250(4), 703-707 (2013).

[Ber2013] A. Bercha, Y. Ivonyak, M. Klimczak, F. Dybala, B. Piechal, W. A. Trzeciakowski, E. Dabrowska, M. Teodorczyk, A. Malag, "Leakage current in 808 nm laser diodes analyzed using high hydrostatic pressure and temperature," physica status solidi (b) 250(4), 769-772 (2013).

[Ber2013a] A. Bercha, B. Piechal, F. Dybala, M. Klimczak, Y. Ivonyak, W. A. Trzeciakowski, "Photoreflectance and photocurrent measurements using pressure tuned laser diodes," physica status solidi (b) 250(4), 708-710 (2013).

[Ber2014] A. Bercha, F. Dybala, B. Piechal, Y. Ivonyak, M. Klimczak, W. A. Trzeciakowski, "Pressure tuning of laser diodes in the near-infrared up to 1850 nm: Operational characteristics and reliability studies," Review of Scientific Instruments 85(6), 063107 (2014).

c) Research papers published before obtaining of the PhD degree

The list includes only research papers published in scientific journals included on the list of the *Journal Citation Reports*.

1. Klimczak, M., Malinowski, M., Sarnecki, J., Piramidowicz, R., Luminescence properties in the visible of Dy:YAG/YAG planar waveguides (2009) Journal of Luminescence, 129 (12), pp. 1869-1873. DOI: 10.1016/j.jlumin.2009.04.073

2. Piramidowicz, R., Bok, A., Klimczak, M., Malinowski, M., UV emission properties of thulium-doped fluorozirconate glasses, (2009) Journal of Luminescence, 129 (12), pp. 1874-1877. DOI: 10.1016/j.jlumin.2009.04.090

3. Klimczak, M., Malinowski, M., Piramidowicz, R., Orange and IR to violet up-conversion processes in Nd:ZBLAN glasses, (2009) Optical Materials, 31 (12), pp. 1811-1814. DOI: 10.1016/j.optmat.2008.12.039

4. Malinowski, M., Kaczkan, M., Klimczak, M., Piramidowicz, R., Ultraviolet emission excitation in RE3+ activated fluoride fibers, (2009) Optical Materials, 31 (3), pp. 484-489. DOI: 10.1016/j.optmat.2007.11.034

5. Piatkowski, D., Wisniewski, K., Koepke, C., Piramidowicz, R., Klimczak, M., Malinowski, M., Initial state-resolved excited state absorption spectroscopy of ZBLAN:Ho3+ glass, (2008) Applied Physics B: Lasers and Optics, 93 (4), pp. 809-816. DOI: 10.1007/s00340-008-3245-6

6. Piatkowski, D., Wisniewski, K., Rozanski, M., Koepke, Cz., Kaczkan, M., Klimczak, M., Piramidowicz, R., Malinowski, M., Excited state absorption spectroscopy of ZBLAN:Ho3+ glass-experiment and simulation, (2008) Journal of Physics Condensed Matter, 20 (15), art. no. 155201. DOI: 10.1088/0953-8984/20/15/155201

7. Piramidowicz, R., Klimczak, M., Malinowski, M., Short-wavelength emission analysis in Dy:ZBLAN glasses, (2008) Optical Materials, 30 (5), pp. 707-710. DOI: 10.1016/j.optmat.2007.02.010

8. Piramidowicz, R., Witoński, P., Klimczak, M., Malinowski, M., Analysis of up-converted UV fluorescence dynamics in Nd^{3+} doped ZBLAN glasses,(2006) Optical Materials, 28 (1-2), pp. 152-156. DOI: 10.1016/j.optmat.2004.10.037

d) Research papers published after obtaining of the PhD degree
The list includes only research papers published in scientific journals included on the list of the *Journal Citation Reports*. The list includes papers contained in the applicant's cycle of research papers related in scope and subject.

1. Buczyński, R., Klimczak, M., Stefaniuk, T., Kasztelanic, R., Siwicki, B., Stępniewski, G., Cimek, J., Pysz, D., Stępień, R., Optical fibers with gradient index nanostructured core, (2015) Optics Express, 23 (20), pp. 25588-25596. DOI: 10.1364/OE.23.025588

2. Siwicki, B., Klimczak, M., Soboń, G., Sotor, J., Pysz, D., Stępień, R., Abramski, K., Buczyński, R. Numerical simulations of spectral broadening in all-normal dispersion photonic crystal fiber at various pump pulse conditions (2015) Optical Engineering, 54 (1), art. no. 016102. DOI: 10.1117/1.OE.54.1.016102

3. Siwicki, B., Klimczak, M., Stępień, R., Buczyński, R., Supercontinuum generation enhancement in all-solid all-normal dispersion soft glass photonic crystal fiber pumped at 1550 nm, (2015) Optical Fiber Technology, 25, pp. 64-71. DOI: 10.1016/j.yofte.2015.08.001

4. Swat, M., Salski, B., Karpisz, T., Stepniewski, G., Kujawa, I., Klimczak, M., Buczynski, R., Numerical analysis of a highly birefringent microstructured optical fiber with an anisotropic core, (2015) Optical and Quantum Electronics, 47 (1), pp. 77-88. DOI: 10.1007/s11082-014-9984-1

5. Cimek, J., Stępień, R., Klimczak, M., Kujawa, I., Pysz, D., Buczyński, R., Modification of borosilicate glass composition for joint thermal processing with lead oxide glasses for development of photonic crystal fibers, (2015) Optical and Quantum Electronics, 47 (1), pp. 27-35. DOI: 10.1007/s11082-014-0011-3

6. Stępniewski, G., Pniewski, J., Klimczak, M., Martynkien, T., Pysz, D., Stępień, R., Kujawa, I., Borzycki, K., Buczyński, R., Broadband dispersion measurement of photonic crystal fibers with nanostructured core, (2015) Optical and Quantum Electronics, 47 (3), pp. 807-814. DOI: 10.1007/s11082-014-9979-y

7. Karpisz, T., Salski, B., Szumska, A., Klimczak, M., Buczynski, R., FDTD analysis of modal dispersive properties of nonlinear photonic crystal fibers, (2015) Optical and Quantum Electronics, 47 (1), pp. 99-106. DOI: 10.1007/s11082-014-9987-y

8. Pysz, D., Kujawa, I., Stepien, R., Klimczak, M., Filipkowski, A., Franczyk, M., Kociszewski, L., Buzniak, J., Harasny, K., Buczynski, R., Stack and draw fabrication of soft glass microstructured fiber optics, (2014) Bulletin of the Polish Academy of Sciences: Technical Sciences, 62 (4), pp. 667-682. DOI: 10.2478/bpasts-2014-0073

9. Klimczak, M., Komolibus, K., Piwoński, T., Siwicki, B., Pysz, D., Stępień, R., Ochalski, T., Buczyński, R., Impact of steepness of pump temporal pulse profile on spectral flatness and correlation of supercontinuum in all-solid photonic crystal fibers with flattened normal dispersion, (2014) Journal of Optics (United Kingdom), 16 (8), art. no. 085202. DOI: 10.1088/2040-8978/16/8/085202

10. Stepien, R., Cimek, J., Pysz, D., Kujawa, I., Klimczak, M., Buczynski, R., Soft glasses for photonic crystal fibers and microstructured optical components, (2014) Optical Engineering, 53 (7), art. no. 071815. DOI: 10.1117/1.OE.53.7.071815

11. Stepniewski, G., Klimczak, M., Bookey, H., Siwicki, B., Pysz, D., Stepien, R., Kar, A.K., Waddie, A.J., Taghizadeh, M.R., Buczynski, R., Broadband supercontinuum generation in normal dispersion all-solid photonic crystal fiber pumped near 1300 nm, (2014) Laser Physics Letters, 11 (5), art. no. 055103. DOI: 10.1088/1612-2011/11/5/055103

12. Klimczak, M., Stepniewski, G., Bookey, H., Szolno, A., Stepien, R., Pysz, D., Kar, A., Waddie, A., Taghizadeh, M.R., Buczynsk, R., Broadband infrared supercontinuum generation in hexagonal-lattice tellurite photonic crystal fiber with dispersion optimized for pumping near 1560 nm: Reply, (2014) Optics Letters, 39 (8), p. 2241. DOI: 10.1364/OL.39.002241

13. Klimczak, M., Soboń, G., Abramski, K., Buczyński, R., Spectral coherence in all-normal dispersion supercontinuum in presence of Raman scattering and direct seeding from sub-picosecond pump, (2014) Optics Express, 22 (26), pp. 31635-31645. DOI: 10.1364/OE.22.031635

14. Kujawa, I., Kasztelanic, R., Stępień, R., Klimczak, M., Cimek, J., Waddie, A.J., Taghizadeh, M.R., Buczyński, R., Optimization of hot embossing method for development of soft glass microcomponents for infrared optics, (2014) Optics and Laser Technology, 55, pp. 11-17. DOI: 10.1016/j.optlastec.2013.06.036

15. Stepien, R., Franczyk, M., Pysz, D., Kujawa, I., Klimczak, M., Buczynski, R., Ytterbium-phosphate glass for microstructured fiber laser, (2014) Materials, 7 (6), pp. 4723-4738. DOI: 10.3390/ma7064723

16. Klimczak, M., Siwicki, B., Skibiński, P., Pysz, D., Stępień, R., Heidt, A., Radzewicz, C., Buczyński, R., Coherent supercontinuum generation up to 2.3μm in all-solid soft-glass photonic crystal fibers with flat all-normal dispersion, (2014) Optics Express, 22 (15), pp. 18824-18832. DOI: 10.1364/OE.22.018824

17. Buczynski, R., Bookey, H., Klimczak, M., Pysz, D., Stepien, R., Martynkien, T., McCarthy, J.E., Waddie, A.J., Kar, A.K., Taghizadeh, M.R., Two octaves supercontinuum generation in lead-bismuth glass based photonic crystal fiber, (2014) Materials, 7 (6), pp. 4658-4668. DOI: 10.3390/ma7064658

18. Sobon, G., Klimczak, M., Sotor, J., Krzempek, K., Pysz, D., Stepien, R., Martynkien, T., Abramski, K.M., Buczynski, R., Infrared supercontinuum generation in softglass photonic crystal fibers pumped at 1560 nm, (2014) Optical Materials Express, 4 (1), pp. 7-15. DOI: 10.1364/OME.4.000007

19. Stepien, R., Siwicki, B., Pysz, D., Stepniewski, G., Kujawa, I., Klimczak, M., Buczynski, R., Characterization of a large core photonic crystal fiber made of lead-bismuth-gallium oxide glass for broadband infrared transmission, (2014) Optical and Quantum Electronics, 46 (4), pp. 553-561. DOI: 10.1007/s11082-013-9835-5

20. Kasztelanic, R., Kujawa, I., Stępień, R., Cimek, J., Haraśny, K., Klimczak, M., Waddie, A.J., Taghizadeh, M.R., Buczyński, R., Fabrication and characterization of microlenses made of tellurite and heavy metal oxide glass developed with hot embossing technology, (2014) Optical and Quantum Electronics, 46 (4), pp. 541-552. DOI: 10.1007/s11082-013-9811-0

21. Klimczak, M., Siwicki, B., Skibinski, P., Pysz, D., Stepien, R., Szolno, A., Pniewski, J., Radzewicz, C., Buczynski, R., Mid-infrared supercontinuum generation in soft-glass suspended core photonic crystal fiber, (2014) Optical and Quantum Electronics, 46 (4), pp. 563-571. DOI: 10.1007/s11082-013-9802-1

22. Bercha, A., Dybala, F., Piechal, B., Ivonyak, Y., Klimczak, M., Trzeciakowski, W.A., Pressure tuning of laser diodes in the near-infrared up to 1850 nm: Operational characteristics and reliability studies, (2014) Review of Scientific Instruments, 85 (6), art. no. 063107. DOI: 10.1063/1.4881607

23. Klimczak, M., Stepniewski, G., Bookey, H., Szolno, A., Stepien, R., Pysz, D., Kar, A., Waddie, A., Taghizadeh, M.R., Buczynski, R., Broadband infrared supercontinuum generation in hexagonal-lattice tellurite photonic crystal fiber with dispersion optimized for pumping near 1560 nm, (2013) Optics Letters, 38 (22), pp. 4679-4682. DOI: 10.1364/OL.38.004679

24. Buczynski, R., Sobon, G., Sotor, J., Klimczak, M., Stepniewski, G., Pysz, D., Martynkien, T., Kasztelanic, R., Stepien, R., Abramski, K.M., Broadband infrared supercontinuum generation in a soft-glass photonic crystal fiber pumped with a sub-picosecond Er-doped fiber laser mode-locked by a graphene saturable absorber, (2013) Laser Physics, 23 (10), art. no. 105106. DOI: 10.1088/1054-660X/23/10/105106

25. Bercha, A., Ivonyak, Y., Klimczak, M., Dybala, F., Piechal, B., Trzeciakowski, W.A., Dabrowska, E., Teodorczyk, M., Malag, A., Leakage current in 808nm laser diodes analyzed using high hydrostatic pressure and temperature, (2013) Physica Status Solidi (B) Basic Research, 250 (4), pp. 769-772. DOI: 10.1002/pssb.201200646

26. Bercha, A., Piechal, B., Dybala, F., Klimczak, M., Ivonyak, Y., Trzeciakowski, W.A., Photoreflectance and photocurrent measurements using pressure tuned laser diodes, (2013) Physica Status Solidi (B) Basic Research, 250 (4), pp. 708-710. DOI: 10.1002/pssb.201200645

27. Dybala, F., Bercha, A., Klimczak, M., Piechal, B., Ivonyak, Y., Trzeciakowski, W.A., Pressure tuning of high-power laser diodes in the 720-1540nm range, (2013) Physica Status Solidi (B) Basic Research, 250 (4), pp. 703-707. DOI: 10.1002/pssb.201200644
28. Klimczak, M., Piramidowicz, R., UV-violet emission properties of 2F(2) 5/2 energy level of Nd 3+ ions in ZBLAN glass (2012) Applied Physics B: Lasers and Optics, 106 (4), pp. 1019-1025. DOI: 10.1007/s00340-011-4789-4

e) Bibliometric indicators

- Sum impact factor according to JCR and to the year of publishing: **71.73**
- Number of citations after Web of Science (WoS): **159**
- Number of citations excluding self-citations after Web of Science: **112**
- Hirsch Index after Web of Science: **8**

as for 18.12.2015, WoS search criterion:
Web of Science: Author Identifiers: 0000-0002-3110-9792
(applicant's ORCID number)

Mariusz Klimczak